Aus der
Ludwig-Maximilians-Universität München
Helmholtz Zentrum München / Institute of Regeneration Medicine and Biology
Director: Dr. Yuval Rinkevich

Dissertation
zum Erwerb des Doctor of Philosophy (Ph.D.) an der
Medizinischen Fakultät der
Ludwig-Maximilians-Universität zu München

In vivo clonal analysis of mesothelium from development to ageing and healthy to injured conditions

vorgelegt von:

Aydan SARDOGAN

aus:

Istanbul, TURKEY

Jahr:

2022

Mit Genehmigung der Medizinischen Fakultät der

Ludwig-Maximilians-Universität zu München

First evaluator (1. TAC member): Prof. Dr. med. Jürgen Behr

Second evaluator (2. TAC member): Dr. Yuval Rinkevich

Dean: **Prof. Dr. med. Thomas Gudermann**

Datum der Verteidigung:

03.07.2023

Affidavit

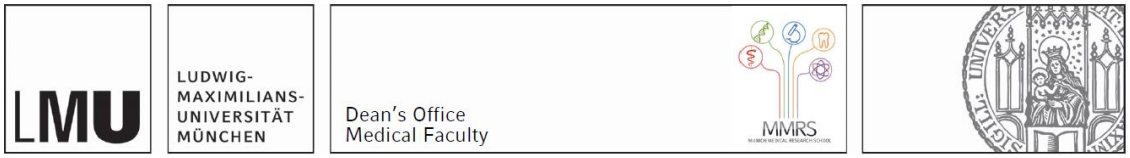

Affidavit

Sardogan, Aydan

Surname, first name

Germany

Country

I hereby declare, that the submitted thesis entitled:

In vivo clonal analysis of mesothelium from development to ageing and healthy to injured conditions

is my own work. I have only used the sources indicated and have not made unauthorised use of services of a third party. Where the work of others has been quoted or reproduced, the source is always given.

I further declare that the dissertation presented here has not been submitted in the same or similar form to any other institution for the purpose of obtaining an academic degree.

Munich,10.07.2023 — place, date

Aydan Sardogan — Signature doctoral candidate

Confirmation of congruency

LMU LUDWIG-MAXIMILIANS-UNIVERSITÄT MÜNCHEN | Dean's Office Medical Faculty | MMRS

Confirmation of congruency between printed and electronic version of the doctoral thesis

Sardogan, Aydan

Surname, first name

Germany

Country

I hereby declare, that the submitted thesis entitled:

In vivo clonal analysis of mesothelium from development to ageing and healthy to injured conditions

is congruent with the printed version both in content and format.

Munich, 10.07.2023 — Aydan Sardogan

place, date — Signature doctoral candidate

Table of content

Abstract (English):

The mesothelium is an epithelial tissue which covers all the internal organs and their cavities in which they abode. The mesothelium is a specialized epithelial monolayer that derives from the embryonic mesoderm germ layer during embryonic development. Ontologically, the organ-covering mesothelium develops between 8- and 18-days post gestation in mouse. In humans, the organ-covering mesothelium develops around day 14 and is at this time-point that mesothelial cells gradually differentiate from round or cuboidal cells to elongated, flattened cells. It is unknown whether the mesothelial-derived mesenchyme that has been laid out during development is being maintained by a mesothelial source, and how it dynamically changes upon injury. Several transgenic mouse lines, developed to genetically trace the surface mesothelium in adult life (e.g. $MSLN^{CreER}$ and $WT1^{CreER}$), inaccurately label other cells or tissues, which restricts their use to study mesothelium development and physiology. In this study, inducible CreER knock-in reporter mouse lines were used that specifically label visceral and parietal mesothelium upon tamoxifen administration. I probed systematically the mesothelium in healthy and injured conditions to unveil its cellular heterogeneity, and its role in tissue maintenance and repair. Our data demonstrates that the mesothelial cells during adult stage does not cause cell clonality nor EMT transition. On the contrary, during post-natal developmental stage, I observed an increase in mesothelial cell clonality. Upon lung fibrosis, abdominal fibrosis, and inflammation, I observed an increase in mesothelial cell clonality and further observed the migration of mesothelial cells to the injured sites to induce repair response. In conclusion, mesothelial cells are important cell constituents needed to maintain organ growth, homeostasis, and injury responses.

List of figures

List of tables

List of abbreviations

APC	Adenomatous polyposis coli protein
DNA	Deoxyribonucleic acid
ECM	Extracellular matrix
EGF	Epidermal growth factor
EMT	Epithelial to mesenchymal transition
EPCR	Endothelial cell protein C receptor
ER	Estrogen receptor
FSMCs	Fibroblasts and smooth muscle cells
GATA4	GATA Binding Protein 4
IPF	Idiopathic pulmonary fibrosis
MMT	Mesothelial to mesenchymal transition
MSLN	Mesothelin
Notch1	Neurogenic locus notch homolog protein 1
PAMPs	Pathogen-associated patterns
PDGF	Platelet-derived growth factor
PDPN	Podoplanin
PMCs	Pleural mesothelial cells
Procr	Protein C receptor
TBX18	T-Box Transcription Factor 18
TF	Tissue factor
TGF-β	Transforming growth factor beta
WT1	Wilms tumor protein 1
α-SMA	Alpha smooth muscle actin

1. Introduction

1.1 The Mesothelium

1.1.1 Introduction to the mesothelium/mesothelial cells

Internal organs in vertebrates arrange in body cavities lined by mesothelium. The mesothelium is the largest epithelium of the body plan and is composed of a monolayer of mesothelial cells that originate from the mesoderm germ layer (Ishihara, Tokuhiro; Ferrnas, Victor J; Jones, Michael; Boyce, Steven; Kawanami, Oichi; Roberts, 1980; Koopmans & Rinkevich, 2018; Wang, 1974). These cavities are lined on the organ surface side and are called visceral mesothelium such as pleura that coats lungs, the pericardium that covers the heart, and the mesentery, but also coat the cavities in which they are called parietal mesothelium, such as peritoneum that encase abdominal digestive and reproductive organs (Koopmans & Rinkevich, 2018; Steven E. Mutsaers, 2002, 2004). The two partitioned mesothelium layers are separated by a serosa fluid interface (Steven E. Mutsaers, 2002). During mouse foetal development, the mesothelium forms between 8-18 days from the lateral plate mesodermal tissue. Around day 14, mesothelial cells transition from round or cuboidal cells into elongated flattened cells (Hesseldah,H; Larsen, 1969; Tiedemann, 1976).

Despite their mesodermal origin, mesothelial cells show both epithelial and mesenchymal cell characteristics such as expression of epithelial cytokeratin 14 and cytokeratin 18 proteins as well as mesenchymal filaments including vimentin and desmin (Ferrandez-lzquierdo, A M.D.; Navarro-Fos, S. M.D.; Gonzalez-Devesa, M. M.D.; Gil-Benso, R. Ph.D.; Llombart-Bosch, 1994). Alike epithelial cells, mesothelial cells present a luminal surface covered by well-developed microvilli that border neighbouring mesothelial cells forming cell-cell junctional complexes, such as tight junctions, adherens junctions, gap junctions, and desmosomes (Steven E. Mutsaers, 2004). In contrast, unlike epithelial cells, mesothelial cells possess a slow turnover with only 0.16-0.5% of the cell population dividing at any given time. However, mitotic activity increases upon injury. For instance, injury to the serosa surface triggers DNA replication in 30-80% of mesothelial cells within

the first 48 hours. Proliferation may be triggered by contact inhibition and soluble mediators from inflammatory and injured cells (Steven E. Mutsaers, 2002).

1.1.2 Mesothelial cell function

Similar to an epithelium, mesothelial cells regulate the transport of fluid and cells across the serosa acting as a semi-impermeable membrane (Steven E. Mutsaers, 2004). Openings at the junctions of mesothelial cells are termed stomata (Von Recklinghausen, 1863). Over the omental milky spot and peritoneal side of organs like diaphragm contains stomatal openings (Mironov et al., 1979) between 3-12µm in diameter (Steven E. Mutsaers, 2002). These openings provide migration paths for immune cells like lymphocytes (Mironov et al., 1979) and removal of cells, bacteria, and particles from the serosa fluid (Steven E. Mutsaers, 2002).

Mesothelial cells act as a barrier against pathogens and display multiple pattern-recognition receptors like Toll-like receptors, nucleotide-binding oligomerization domain like receptors (RIG-I-like receptors), and C-type lectin-like receptors. These receptors recognize carbohydrates and lipopolysaccharides on the surface of microbial pathogens like bacteria, fungi and viruses and release inflammatory mediators in response to initiate inflammation. Toll-like receptors also recognizes the pathogen-associated patterns (PAMPs) to innate immune responses. Recognition of PAMPs also stimulates the secretion of cytokines and cell growth (Jantz & Antony, 2008).

Mesothelial cells also maintain serosa homeostasis by generating a frictionless interface that ensures free-range movements between opposing organs and tissues (Figure 1) (Steven E. Mutsaers, 2002). For this, mesothelial cells synthesise a non-adhesive lubricant formed by diverse phospholipids, proteoglycans, and glycosaminoglycans, which together form the surface glycocalyx.

Besides its function as a natural lubricant, the glycocalyx might influence mesothelial cell function via its interaction with the microvilli. Microvilli concentration on mesothelial cells vary between different organs, adjacent cells, and depending on the physiological context (S. E. Mutsaers, Whitaker, & Papadimitriou, 1996).

Mesothelial microvilli increase the surface area of the cells (Odor, 1954) facilitating membrane dependent metabolic activities, protecting serosal surfaces from damage, and trapping serosal secretions (S. E. Mutsaers et al., 1996). The function of microvilli remains poorly understood, but it has been hypothesized that it might alter the glycocalyx secretion upon injury. Due to the change of cell surface charge, glycocalyx composition may be also reflected (Gotloib, L; Shostack, A; Jaichenko, 1988). Glycocalyx covered microvilli also includes glycosaminogylcans to bind fluids and drive the absorption (Wang, 1974). Secreted gycosaminogylcans by mesothelial cells are mostly hyaluronan (Roth, 1973) and locally produced (Arai, H; Endo, M; Sasai, 1975). Synthesis of hyaluronan protects the formation of adhesions and inhibits spreading of tumour cells and growing (Jones et al., 1995).

Mesothelial cells also play direct roles in initiation and resolving serosal inflammation and repair in response to injury. They secrete pro- and anti- immunomodulatory mediators including products of the coagulation cascade, chemokines, cytokines, prostaglandins and prostacyclin, reactive oxygen species, and antioxidant enzymes (Steven E. Mutsaers et al., 2002). Serosal inflammation begins at the surface of the mesothelial cells by releasing chemokines. Chemotactic gradients from the basolateral to the apical side of the mesothelial cell is created by secretion of chemokines towards to the apical surface (Li et al., 1998). Immune cells follow this gradient and get through the mesothelial cell monolayers through the stomata (Steven E. Mutsaers, 2002).Upon injury, mesothelial cells release factors to induce cell-proliferation, migration and ECM synthesis. These processes are orchestrated by growth factors like transforming growth factor beta (TGF-β), platelet-derived growth factor (PDGF), fibroblast growth factor, hepatocyte growth factor, and members of epidermal growth factor (EGF) (S. E. Mutsaers et al., 1997). Furthermore, mesothelial cells synthesize ECM molecules, collagen types I, III, IV, elastin, fibronectin and laminin (Rennard et al., 1984). In addition, mesothelial cells regulate ECM turnover by secreting matrix metalloproteinases and tissue inhibitor of metalloproteinases (Steven E. Mutsaers, 2004) (Figure 2). Local fibrin deposition and clearance within serosal cavities is another essential role of mesothelial cells. Fibrinolytic activity prevents

and removes fibrin deposits that are formed upon mechanical injury, hemothoraces and infection (Holmdahl, 1997).

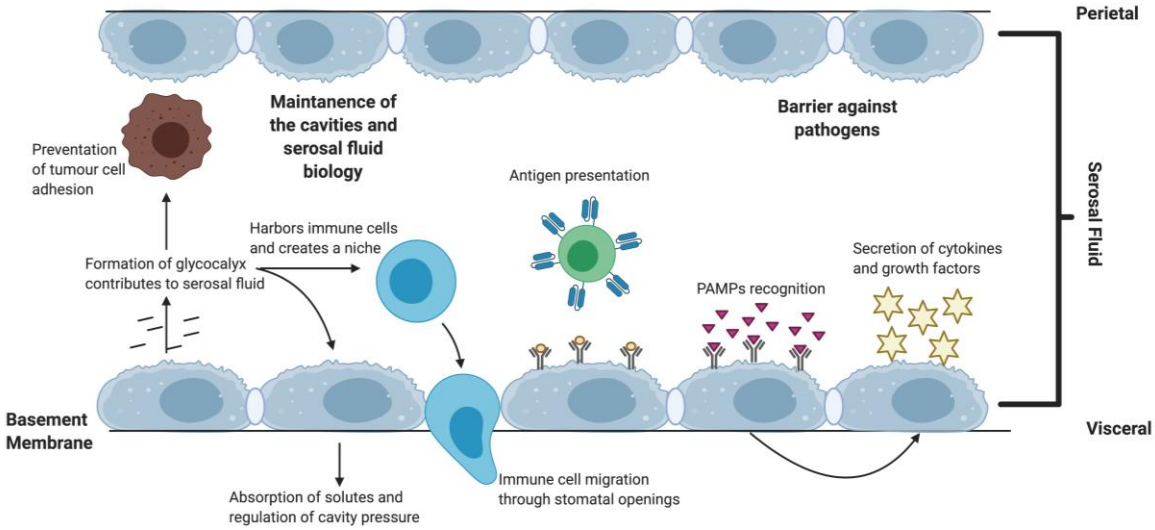

Figure 1 : Role of mesothelial cells. Mesothelium maintains serosal integrity and function. Mesothelial cells have a protective role as they provide a physical barrier against invading pathogens and immune cells as well as recognizing pathogen-associated molecular partners (PAMPs). By secreting glycocalyx, they create chemotactic gradient that initiate immune-response and cell migration through the stomatal openings. Glycocalyx secretion by mesothelium also inhibits cancer cell migration and proliferation within the body cavities. This protective barrier provides a slippery, non-adhesive surface to allow organs to move freely within the cavities. Mesothelium facilitates transport of fluid and cells across the serosal cavities. This fluid can contain antigens and cytokines, growth factors, ECM, proteases, and other inflammatory mediators. These molecules participate in the induction and resolution of inflammation and tissue repair (Created with Biorender.com).

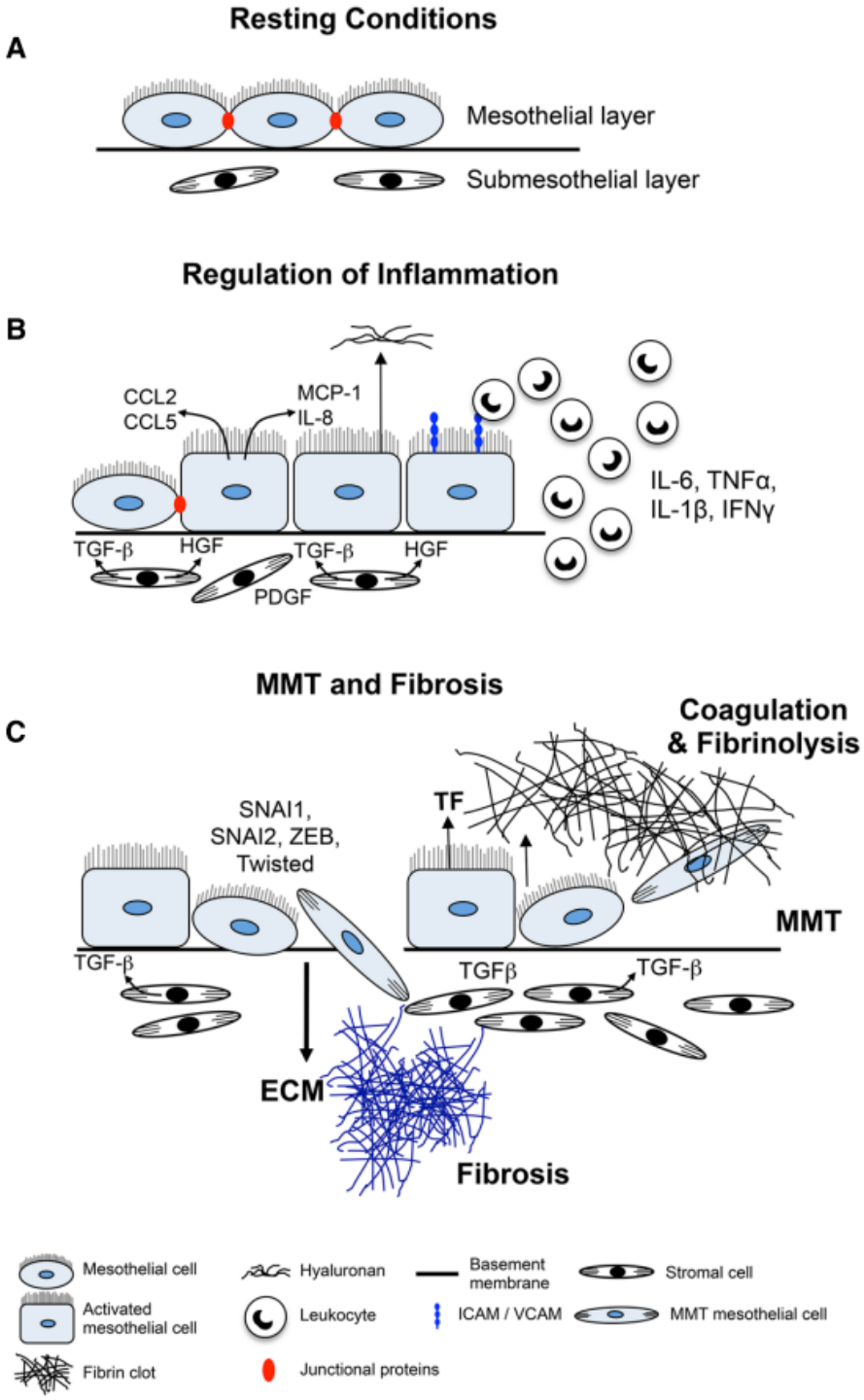

Figure 2: Mesothelial cell mechanism upon injury. (A) Mesothelial cells under homeostasis under resting on the basement membrane. (B) Mechanism of mesothelial cells under inflammation. They are secreting inflammatory mediators, chemokines, growth factors. Under the inflammatory phase they become cubical shape and lose the cell-cell connection. (C) Mechanism of mesothelial cells under fibrosis and MMT. For coagulation and matrix deposition they are secreting tissue factor (TF). Published under Frontiers in Pharmacology. 2015, Licensed 4.0 BY (Steven E. Mutsaers et al., 2015).

Interestingly, embryonic mesothelium also serves as a tissue source for interstitial fibroblasts and vascular smooth muscle cells (VSMCs) which have a major role in development, physiology, and pathology of internal organs (Rinkevich et al., 2012). This is facilitated as mesothelial cells remain just partially differentiated while maintaining their capacity to change their phenotype, especially during development and injury (Herrick & Mutsaers, 2004). Studies in mice indicate that during development, mesothelium lining the gut, liver, and heart differentiate into vascular smooth muscle via epithelial-to-mesenchymal transition (EMT), during which mesothelial cells lose their epithelial-like structures and properties (Munoz-Chapuli, R; Perez-Pomares, JM; Macias, 1999; Perez-Pomares et al., 2002; Pérez-Pomares et al., 2004). Normally, epithelial cells express high level of E-cadherin while mesenchymal cells express high level of N-cadherin, fibronectin, and vimentin. Therefore, during the EMT, loss of E-cadherin and up-regulation of N-Cadherin, fibronectin and vimentin occurs in mesothelial cells (Kalluri & Weinberg, 2009).

1.2 Mesothelium during development

Adult mesothelium originates from the coelomic epithelium, an embryonic precursor that originates from the binary division of the lateral plate mesoderm (Moore, K., Persaud, T. & Torchia, 2019). During this process, the cells forming the coelomic epithelium already exhibit features of epithelial cells, such as association to a basal lamina and baso-apical polarization. They also contribute significantly to organ development by undergoing EMT and giving rise to different cell types such as fibroblasts and smooth muscle cells (Figure 3) (Koopmans & Rinkevich, 2018; Moore, K., Persaud, T. & Torchia, 2019). The capacity to differentiate via EMT into mesenchymal populations transcend into adult stages to support tissue repair caused by fibrosis, adhesions, ischemia, infarctions, and cancer (Koopmans & Rinkevich, 2018).

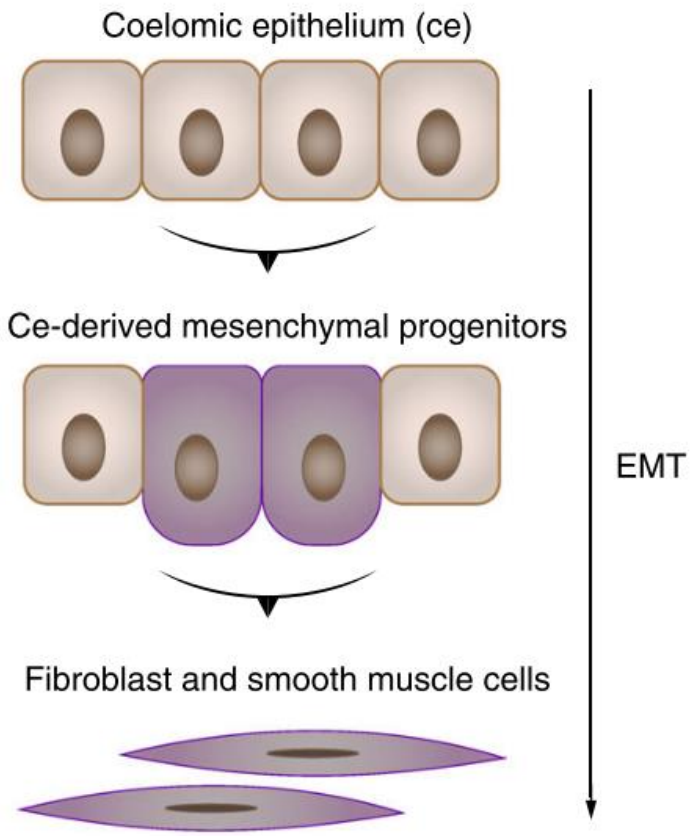

Figure 3: Differentiation of coelomic epithelium during organ development. (Reproduced from Tim Koopmans and Yuval Rinkevich. Published under Communications Biology 2018, License CC by 4.0 (Koopmans & Rinkevich, 2018))

To study mesothelial cells, marker genes WT1, TBX18, MSLN, Notch1, and GATA4 (Figure 4) (Koopmans & Rinkevich, 2018) have been used to trace embryonic and adult mesothelial precursors. Lineage tracing of peritoneal mesothelium shows that cell proliferation and clonal expansion is highly active during postnatal development (Wilm et al., 2021) and after injury in post-surgical adhesions (Fischer et al., 2020). These studies indicate that mesothelial cells act as self-renewing stem cells that function as progenitors for smooth muscle and fibroblasts during organ development, growth, and repair.

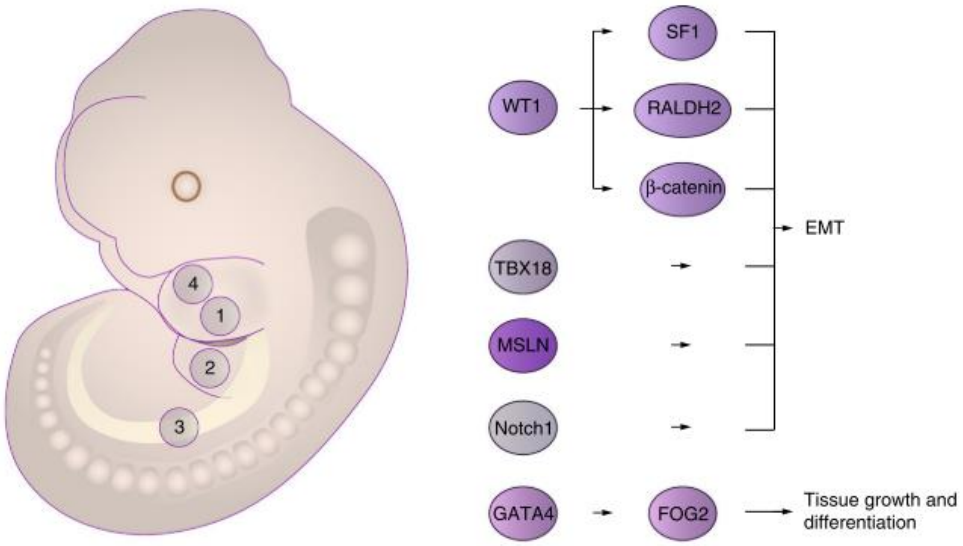

Figure 4: Genes involve mesothelial to mesenchymal transition (MMT) during development. (1) Heart, (2) Liver, (3) Gonads, (4) Lungs. Common set of genes, WT1, TBX18, MSLN, Notch1, GATA4 with their downstream genes. These set of genes supports EMT during development. (Reproduced from Tim Koopmans and Yuval Rinkevich. Published under Communications Biology 2018, License CC by 4.0 (Koopmans & Rinkevich, 2018))

1.3 Basement Membrane

The basement membrane is composed of four major components such as type IV collagen, laminins, entactin, and heparin sulfate proteoglycans. Out of these, type IV collagen comprises of about 50% of the total composition. Injury to the basement membrane elicits cellular remodeling that leads to the deposition of new basement membrane proteins, which further initiates repair response such as fibroblast activation and immune cells recruitment (Horejs, 2016; LeBleu et al., 2007).

The basement membrane is a thin, dense, cell-adherent, sheet-like extracellular matrix that is widely distributed in tissues and organs (Pozzi et al., 2017; Zheng & Yamada, 2019). Basement membrane lies below the epithelial cell layers, such as the mesothelium and they underly the connective tissue which consists of matrix, capillaries, and fibroblasts (Figure 5).

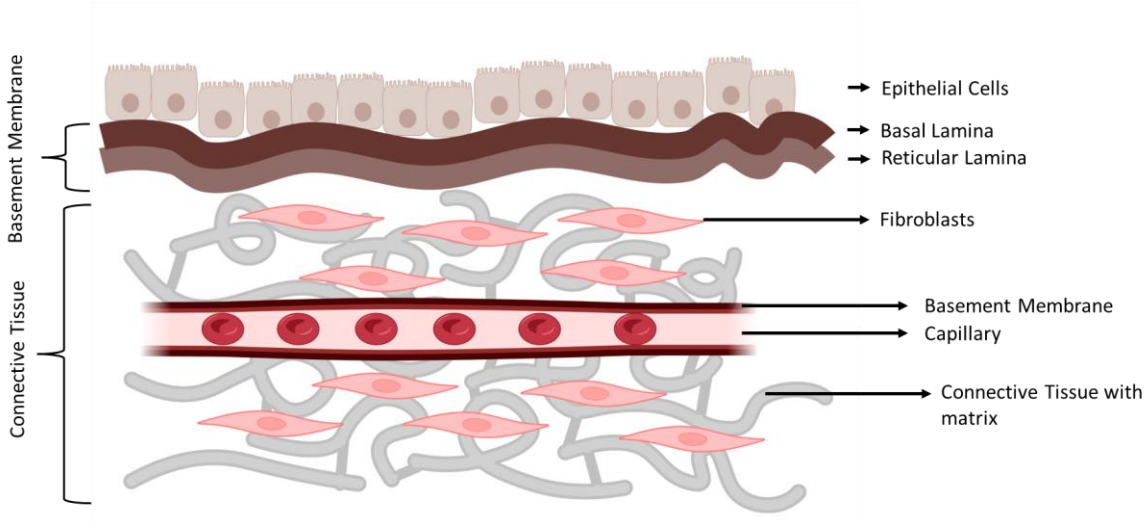

Figure 5: Illustration of basement membrane. (Created by Biorender.com)

Mesothelial cells attach loosely to the basement membrane (Steven E. Mutsaers, 2002) via Integrin β-1 (CD29) (Lachaud et al., 2013, 2015). Under injury or trauma, mesothelial cells detach from the basement membrane (Raftery, 1973). Basement membrane is important to keep mesothelial cells intact to the organ surface and contributing to mesothelial cell homeostasis. Importance of basement membrane and mesothelial cell relation is not studied yet. It has been only known that upon injury mesothelial cells may detach from the basement membrane to become free floating cells (Herrick & Mutsaers, 2004).

Interaction between mesothelial cells and basement membrane is poorly investigated. However, the integrity and clonality of mesothelium lining is directly linked to basement membrane signals and is one of the focuses of this thesis.

1.4 Mesothelium related pathologies

Besides the many protective roles of mesothelium, mesothelial cells also mediate pathologies such as postsurgical adhesions and fibrosis ((Steven Eugene Mutsaers et al., 2016).

1.4.1 Post-surgical adhesions

Post-surgical intra-abdominal adhesions are pathological fibrous bands that develop between and attach two opposing organ surfaces. These types of pathological fibrous bands contain nerve tissue and blood vessel which are derived from thin lamella of connective tissue or thick fibrous bridges (Braun & Diamond, 2014; Herrick & Wilm, 2021). Certain types of adhesions are congenital but more commonly form as a response to trauma. Myomectomy, endometriosis- ovarian- and tubal-surgery like gynaecologic operations are high-risk procedures (>80%) concerning adhesion development. Adhesions can also occur in the presence of intra-peritoneal inflammation, such as appendicitis (Steven Eugene Mutsaers et al., 2016).

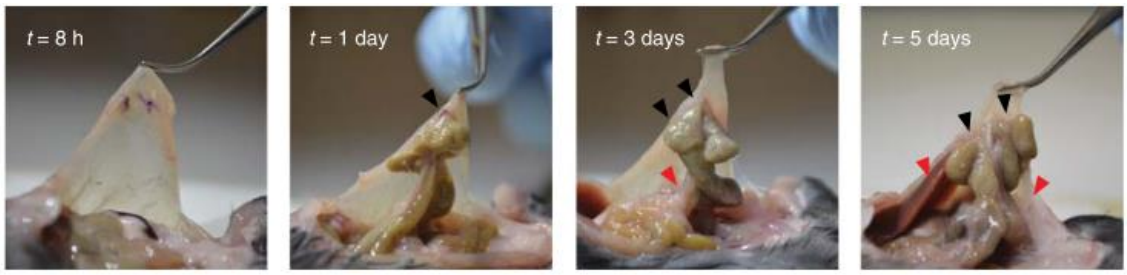

Figure 6: Formation of adhesion over time between peritoneum and caecum in mice. Black arrow represents the adhesion occurring between caecum and peritoneum, red arrow represents the other organs joining the adhesion site. (Reproduced from Adrian Fischer, Tim Koopmans et al, Yuval Rinkevich. Published under Nature Communication 2020, License CC by 4.0 (Fischer et al., 2020))

It has been hypothesized that the formation of adhesions is the result of serosanguinous exudate leakage from injured serosa that is rich in fibrin (Holmdahl, 1997). Trauma induces release of cytokines and chemokines TNF-α, IL-6, and IL-8 within the peritoneal cavity (Badia et al., 1996) (Section 1.1.2 and Figure 1).

These compounds attract neutrophils and activate mesothelial cells and macrophages. These molecules lead to additional leakage of fibrin (Menzies & Ellis, 1990) that in turn causes severe, chronic organ dysfunction. These complications increase the need of additional surgeries to prevent or separate the adhesion sites between organs (Herrick & Wilm, 2021).

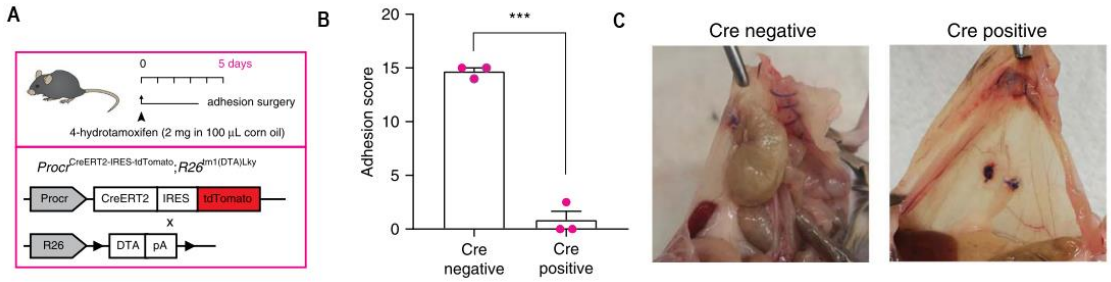

Figure 7: Formation of post-surgical adhesion in the absence of mesothelial cells. (A) Transgenic mouse model to deplete mesothelial cells under the mesothelial specific promoter ProcrCreER x DTA. (B) Adhesion score in the absence (Cre positive) and in the presence (Cre negative) of mesothelial cells. (C) Adhesion formation between peritoneum and caecum in the absence and presence of mesothelial cells. (Reproduced from Adrian Fischer, Tim Koopmans et al, Yuval Rinkevich. Published under Nature Communication 2020, License CC by 4.0 (Fischer et al., 2020))

In vivo method to study surgical adhesions published in our lab, after 5 days of post-surgery to induce adhesion between opposing caecum and peritoneum organs stick to each other to form adhesion (Figure 6). In this study, depletion of mesothelial cells inhibited adhesion formation, and this showed us the importance of mesothelium on the formation and preventing of post-surgical adhesions (Figure 7). Therefore, their tracing studies are still remaining unstudied, and it is important to understand their role in post-surgical adhesions.

1.4.2 Idiopathic pulmonary fibrosis (IPF)

IPF is a progressive lung disease where lungs abnormally accumulate collagen-enriched extracellular matrix, causing breathing difficulties. The structural and cellular changes of the lung parenchyma into a scar-type tissue are believed to be caused by myofibroblasts (Kaminski et al., 2003; Mubarak et al., 2012). Myofibroblasts are a fibroblast subpopulation activated during fibrosis and characterized by the expression of alpha smooth muscle actin (α-SMA) (Kalluri & Neilson, 2003). However, the cellular origin of these scar-forming cells remain largely unknown (Habiel, David M; Hogaboam, 2017; Liu et al., 2020; Mubarak et al., 2012).

During IPF, pleural mesothelial cells have the potential to migrate into the lungs and transit into a myofibroblast phenotype (Mubarak et al., 2012; Zolak et al., 2013). It is well known that mesothelial cells under stress conditions undergo EMT, reduce expression of mesothelial cell markers, and adherens junctional proteins such as N-cadherin, E-cadherin and Cytokeratin (Mubarak et al., 2012). Additionally, mesothelial cells secrete high levels of TGF-β during parenchymal

inflammation, which is considered as a key driver of EMT and fibrosis (Habiel, David M; Hogaboam, 2017; Nasreen et al., 2009). Therefore, mesothelial cells play important roles in IPF, working as a source for myofibroblasts and coordinating fibrosis-related signals.

Lineage tracing of mesothelium under IPF conditions are poorly studied, therefore pleural cavity, lungs and heart lined by the mesothelium. Upon lung injury, mesothelium is the first layer of cells getting affected and highlight the significance of mesothelial lining in fibrosis initiation.

Aim and hypotheses of the project

Mesothelial cells are one of the biggest epithelial organs in mammalians which cover all the organs surfaces and cavities. Their role as progenitors for mesenchymal populations during organ development, growth, and repair makes very important to understand how the self-renewal and differentiation potential of this population is changed/maintained during different ontological stages of mesothelium.

We have 5 aims in this Thesis,

- ✓ Investigation of the self-renewal capacity of the adult mesothelium
- ✓ Investigation of the self-renewal capacity of the neonatal mesothelium.
- ✓ Investigation of the mesenchymal lineage differentiation capacity of the adult mesothelium
- ✓ Establishing behaviour of mesothelium in various injury models in adult life
- ✓ Importance of basement membrane on mesothelial cell behaviour

2. Material and Methods

2.1 Mice

All mouse strains, (PDPNCreER, ProCrCreER, mT/mG, Ai14) were either obtained from Jackson laboratories, or generated at the Stanford University Research Animal Facility, and were housed at the Helmholtz Center Animal Facility. The animal house rooms were maintained at constant temperature and humidity with a 12-h light cycle. Animals were allowed food and water ad libitum. All animal experiments were reviewed and approved by the Government of Upper Bavaria (TVA numbers ROB-55.2-2532.Vet_02-18-62, ROB-55.2-2532.Vet_02-20-216, ROB-55.2-2532.Vet_02-17-97 and ROB-55.2-2532.Vet_02-19-101).

2.2 Mice genotyping

Genotyping was performed to distinguish mouse lines containing 190-base pair (bp) (PDPNCreER), 100bp (ProCrCreER) Cre fragment (Cre+/–). The genomic DNA from the ear clips was extracted using QuickExtract DNA extraction solution (Biozym, Cat# 101094) following the manufacturer's guidelines. For the PDPNCreER mice line, DNA extract (1 µl) was added to each 19 µl PCR. The reaction mixture was set up using GoTaq Green Master Mix kit (Promega, Cat# M7123) containing 1X GoTaq green master enzyme mix, 0.5µM forward primer “1318flp-YRI2”-5′ GAT GGG GAA CAG GGC AAG TTG G C-3‴ (Sigma) and 0.5µM reverse primer “1320flp-YRI2”-5′ GGC TCT ACT TCA TCG CAT TCC TTG C -3′ (Sigma). PCRs were performed with initial denaturation for 5 mins at 94°C, amplification for 35 cycles (denaturation for 30 sec at 94°C, annealing for 30 s at 65°C, and elongation for 1 min at 68°C) and final elongation for 10 mins at 68°C, and then cooled to 4°C. For the ProCrCr-ER mice line, DNA extract (1 µl) was added to each 19 µl PCR. The reaction mixture was set up using GoTaq Green Master Mix kit (Promega, Cat# M7123) containing 1X GoTaq green master enzyme mix, 0.5µM forward primer “Cre-FW” ′5-GCG GTC TGG CAG TAA AAA CTA TC GCG GTC TGG CAG TAA AAA CTA TC-3‴ (Sigma) and 0.5µM reverse primer “Cre-RV”-5′ GTG AAA CAG CAT TGC TGT CAC TT-3′ (Sigma). PCRs were performed with initial denaturation for 5 mins at 94°C, amplification for 35

cycles (denaturation for 30 sec at 94°C, annealing for 30 s at 59°C, and elongation for 1 min at 72°C) and final elongation for 10 mins at 72°C, and then cooled to 4°C. In every experiment, negative controls (non-template and extraction) and positive controls were included. The reactions were carried out in life technologies, ProFlex PCR System. Reactions were analyzed by gel electrophoresis.

2.3 Tamoxifen inducible *in vivo* model to investigate clonality of cells

In this study specifically two mouse models specific to mesothelial cells and two reporter lines are used. This model is very useful to study and trace the mesothelial cells specifically on the organ surfaces.

Tamoxifen inducible lines used in this thesis are ProcrCreER and PDPNCreER (surface mesothelial specific markers) for all organs. PDPN is a 43 kDa transmembrane glycoprotein. PDPN plays a key role during development of the heart, brain, kidney, osteoblasts, lung, and lymphoid organs. PDPN undergoes EMT and upregulation of PDPN is corelated with motility and metastasis (Astarita et al., 2012). PDPN is expressed in kidney glomerular epithelial cells (podocytes), epithelial and mesothelial cells such as intestinal epithelium, alveolar type I cells, mesothelium of the visceral peritoneum, and lymphatic endothelium. Procr is N-glycosylated type I membrane protein. Procr was first identified as an endothelial cell protein C receptor (EPCR) as a transmembrane glycoprotein binds to protein C and actives the protein C (APC). Procr is a type 1 transmembrane protein (Rao, L. Vijaya Mohan; Esmon, Charles T.; Pendurthi, 2014). Procr is expressed in endothelial cells, organ surfaces (mesothelium), and ovarian surface epithelium. Reporter lines are used in thesis are mT/mG, Ai14. All cells in mT/mG is red and under the tamoxifen induction PDPN and Procr positive cells turns to green, all cells have no color in Ai14 mouse under the tamoxifen induction PDPN and Procr positive cells turns to red.

Tamoxifen inducible lines are also known as CreER/LoxP systems. Design of the genome of mice is tissue specific promoter is in front of the CreER gene and this mouse is mated with the mouse which has loxP sites. In between this loxP sites

the gene which wanted to knock out takes place and right behind the second loxP site the gene which wanted to be turned on takes place (Figure 8).

Figure 8: Illustrated mating of CreER mouse with mTmG reporter mouse. When the Cre is activated with tamoxifen, gene specific promoter turns the interested gene into green.

The mouse we have in the laboratory are designed with estrogen receptor (ER) that binds to 4-hydrotamoxifen (4-OH tamoxifen) instead of 17β-estradiol. When tamoxifen is administered to the mice, tamoxifen is metabolized to 4-OH tamoxifen that binds to ER and Cre and activates mesothelial cell specific promoter. When cre is activated, it binds to loxP sites flanking, knocking out color of red and changes the color of cell of interest to green (Figure 8 and 9). In this study we used 4-OH tamoxifen instead of tamoxifen, because injection of metabolite takes less time than than the metabolization of tamoxifen.

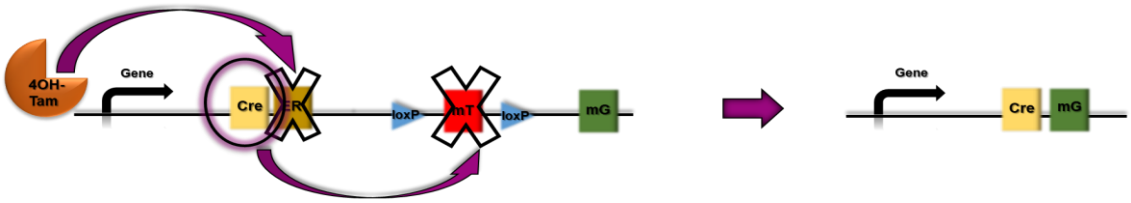

Figure 9: Illustration of how tamoxifen induces CreER system in mouse model. 4-OH tamoxifen binds to ER to release the Cre that Cre can bind to loxP and knockouts the mT.

2.4 Tamoxifen preparation

4-hydrotamoxifen (Sigma Aldrich, Cat# H6278-50mg) were used in all the experiments. First aliquotes were prepared from the 50mg stock 4-hydrotamoxifen powder. 3 mL absolute ethanol was added to the stock bottle containing 50 mg powdered 4-hydrotamoxifen. Solution was vortexed until completely dissolved. The solution was then divided over 1.5 mL Eppendorf tubes. Tubes were placed in a vacuum centrifuge with open lids and centrifuged for 2-4 hours at 45^{o}C until all ethanol was evaporated. The aliquots were stored at -80^{o}C until further use. Desired amount of tamoxifen aliquots was taken and added to 500µL corn oil

(Sigma Aldrich, Cat# C8267-500ML) per aliquot. Tubes were placed in a sonicator and run for 4 times with the following program; where each run took 10 mins, 10 cycle, each cycle 30seconds run and 30 seconds wait. Solutions were stored in the -20 until further use.

2.5 Clonal tracing

6–7-week-old adult PDPNCreER x TM4 mice were injected via intraperitoneal (i.p.) injection with 1mg 4-hydrotamoxifen. Caecum, heart, liver, lung and the peritoneal wall were collected at 7 day, 3-months, 6-months, and 1-year timepoints. ProCrCreER x TM4 mice were injected via i.p. injection with 2mg 4-hydrotamoxifen to 6-7 weeks age old adults. Organs were collected at 7 day, 3-month, 6-month, and 1-year timepoints PDPNCreER x TM4 and ProCrCreER x TM4 P0 pups were injected with 0.125mg 4-hydrotamoxifen and organs were collected at time point's day 2, day 7 and day 30.

2.6 Lineage tracing

PDPNCreER x TM4 mice were injected via i.p. injection with 1mg 4-hydrotamoxifen 3 times (every other day) to 6-7 weeks age old adults. Organs (peritoneal wall, liver (large lobe), cecum, lung and heart) collected at 7 day, 3-month and 6-month, and 1-year timepoints. ProCrCreER x TM4 mice were injected via i.p. injection with 2mg 4-hydrotamoxifen (Sigma, H6278-50mg, dissolved in corn oil) 3 times (every other day) to 6-7 weeks age old adults. Organs collected at time point's 7 day, 3-month, and 6-month, and 1-year timepoints.

2.7 Clonal analysis with inhibitors

P0 pups were injected with 4-OH tam (0.125mg) via subcutaneous (s.c.). Next day group 1 pups were injected with InVivoMAb anti-mouse CD29 (1:400 dilution) (Bio X Cell, Cat# BE0232) and group 2 pups were injected with InVivoMAb anti-mouse CD54 (1:400 dilution) (Bio X Cell,Cat# BE0020-1). Samples were collected at P7. Further 3D staining and images were followed.

2.8 Abdominal fibrosis by surgical adhesions mice

Mice were anesthetized by i.p. injection of Medetomidin (500 µg/kg), Midazolam (5 mg/kg) and Fentanyl (50 µg/kg) cocktail (MMF). Anesthetic depth was monitored and assessed by toe reflex. To avoid dehydration, eyes were covered with Bepanthen, and the abdomen was shaved and disinfected with betadine. Animals were kept on their backs on a heating plate at 39 °C. A midline laparotomy (1–2 cm) was performed through the skin and peritoneum. Four hooks, positioned around the incision and fixed to a retractor and magnetic base plate. The peritoneal surface and opposing cecal surface were brushed gently with a small surgical brush. Serosal surface of the peritoneum was knotted by using 4-0 silk sutures (Ethicon). A dab talc powder (Sigma Aldrich, Cat#243604) was applied gently with a cotton swab onto the injured surfaces. Buprenorphine (0.1 mg/kg) was pipetted in the abdomen before closure of the incision, to allow for initial postsurgical analgesia. Metamizole in drinking water (1,25 ml metamizole/ml) was provided for long term analgesia. The peritoneum and skin were closed with two separate 4-0 silk sutures (Ethicon). Atipamezol (2,5 mg/kg KGW) and Flumazenil (500 µg/kg KGW) were injected as an antagonist to MMF to waken up the mice by subcutaneous injection (s.c.).

2.9 *In vivo* lung inflammation and fibrosis

Mice were anesthetized by an i.p. injection of a Medetomidin (500 µg/kg), Midazolam (5 mg/kg) and Fentanyl (50 µg/kg) cocktail (MMF). Anesthetic depth was monitored and assessed by toe reflex. To avoid dehydration eyes were covered with Bepanthen. Mice were administered with a single dose of Bleomycin sulfate (Sigma Aldrich, Cat# B5507-15UN) in phosphate buffer saline (PBS) in the concentration of 2U/kg via intratracheal instillation Table 1 and Table 2 and control group were administered with a single dose of PBS via intratracheal instillation. Atipamezol (2,5 mg/kg KGW), Flumazenil (500 µg/kg KGW), Naloxon (1200 µg/kg KGW) was injected as an antagonist to MMF to waken up the mice by subcutaneous (s.c.) injection.

Table 1: Calculation of 2U Bleomycin from Stock

		Elastase µl	PBS µl
Used concentration : U/kg mice	2		
Stock (10 mg) resolved in:	1000 µl		
Concentration:	0.015 U/µl		
Volume needed for (number mice=)		0.00	0
Sigma	Cat No: B5507-15U		
Bleomycin			

Table 2: Amount of bleomycin application correlating to mouse weight

Weight	Bleo µl	PBS µl	
20	2.67	77.33	80
21	2.80	77.20	80
22	2.93	77.07	80
23	3.07	76.93	80
24	3.20	76.80	80
25	3.33	76.67	80
26	3.47	76.53	80
27	3.60	76.40	80
28	3.73	76.27	80
29	3.87	76.13	80
30	4.00	76.00	80
31	4.13	75.87	80
32	4.27	75.73	80
33	4.40	75.60	80
34	4.53	75.47	80
35	4.67	75.33	80

2.10 Abdominal inflammation by LPS infection

LPS (Sigma, Cat#L8274) was injected via i.p. after 2days of 4-OH tam injection via i.p. 5 times injection of LPS/DF mix. Samples were collected at day 9.

2.11 Tissue collection

Organs were fixed overnight at 4°C in 2%paraformaldehyde (PFA) (VWR, #43368.9M)/ PBS after organs were excised from mice. Following day, fixed tissues were washed 3 time with PBS and stored in PBS-GT (PBS with 0.2% gelatin (Serve, Cat #23311.01), 0.5% Triton-X (Sigma, Cat#T8784-16), 0.01% thimerosal (Sigma, Cat#X100-100mL)) at 4 °C.

2.12 3D- staining of organs

Whole-mount samples were stained and cleared with a modified 3DISCO protocol (Ertürk et al., 2012). Samples stored in PBS-GT were incubated in anti-GFP (Abcam, Cat#ab13970, 1:500 dilution) and anti-PDPN (Abcam, Cat#ab11936, 1:500 dilution)) primary antibodies for 36 hours at RT while shaking. Organs were then washed vigorously in with PBS-GT with the final wash step overnight at RT while shaking. Then, collected mouse organs were incubated in goat-anti-Chicken-488 (Life Technologies Cat#A-11039, 1:500 dilution) and goat-anti-Hamster-647 (Life Technologies, Cat#A-21451 A-1:500 dilution) antibodies for 36 hours at RT in PBS-GT while shaking. Afterwards organs were washed vigorously in with PBS-GT with the final wash step overnight at RT while shaking. Samples were stored in PBS for further imaging.

2.13 Preparing for Histology

Organs were embedded in O.C.T^{TM} (optimal cutting temperature) Compound Containing (Sakura, Cat#4583) on dry ice and cut using Hyrax C5 cryotome. Prepared slides were stored at -20^{o}C until staining.

2.14 Immunostaining

Samples were permeabilised in ice cold acetone for 3 minutes. Samples were washed with PBS 3 times for 5 minutes and blocked with 200µl of 5%BSA (Sigma Aldrich, Cat# A4503-50G) in PBS at RT for 1 hour. Samples were incubated in primary antibody diluted in 1% BSA in PBS at 4°C overnight. Next day, slides were washed with PBS 3 times for 20 minutes each. Samples were incubated in

secondary antibody diluted in in 1% BSA in PBS at RT for 2 hours. After 2 hours slides were washed 3 times for 20 minutes each and were mounted with Fluoro-mount-GTM with DAPI (LIFE Technologies, Cat#00-4959-52) and stored at 4°C See Table 3 for list of antibodies and dilutions.

Table 3: Antibody list used during immunostaining

Antibodies	**Company**	**Dilution**	**Primary/Secondary**
Syrian Hamster-anti – PDPN	Abcam Cat# ab11936	1:500	Primary
Chicken-anti – GFP	Abcam Cat# ab13970	1:500	Primary
Goat-anti – alpha SMA	Abcam Cat# ab21027	1:250	Primary
Rabbit-anti – Ki67	Abcam Cat# ab16667	1:250	Primary
Rat-anti – CD45	Abcam Cat# ab23910	1:250	Primary
Goat-anti-Hamster-647	Life Technologies Cat# A-21451	1:1000	Secondary
Goat-anti-Chicken-488	Life Technologies Cat# A-11039	1:1000	Secondary
Goat-anti-Rabbit-488	Life Technologies Cat# A11008	1:1000	Secondary
Donkey-anti-Rabbit-647	Life Technologies Cat# A31573	1:1000	Secondary
Goat-anti-Rat-647	Life Technologies Cat# A21247	1:1000	Secondary

2.15 Trichrome Staining

Trichrome staining was done by using Masson trichrome staining kit (Sigma, Cat#HT15-1KT). Samples were fixed with ice cold acetone (-20^{o}C) for 10 minutes, air dried for 5 minutes and washed with deionized water for 2 minutes. Samples were then incubated in 56^{o}C preheated Bouin's Solution (Sigma-Aldrich, Cat# HT10132-1L) for 15 minutes and washed under running tap water until the color is gone. Then slides were incubated in the Weigert's Iron Hematoxylin (Sigma-Aldrich, Cat#HT1079-1SET) solution for 3 minutes at RT and washed under the running tap water until the color is gone. Samples were incubated in the Biebrich Scarled-Acid Fucshin (Schubert und Weiss, Cat# SI HT151-250ML) for 5 minutes at RT and rinsed in deionized water. Afterwards, slides were incubated in working Phosphotungstic/Phosphomolybdic acid solution (45mL of phosphotungstic acid, 45mL of phosphomolybdic acid for and 90mL of deionized water) 5 minutes at RT. They were then transferred to into the Anilline Blue (Schubert und Weiss, Cat# SI B8563-250ML) solution for 10 minutes at RT then rinsed with 1% acetic acid for 2 minutes and rinsed with distilled water. Dehydration was done in 80% ethanol, 2x100% ethanol each for 5 minutes. Clearing was done with Roti-Histol (Roth, Cat# 6640.1). Lastly, slides were mounted with Roti-Histokitt (Broth, Cat#6638.1).

2.16 3D whole-mount microscopy

Samples were imaged in 35-mm glass-bottom dishes (Ibidi, Cat#81218) using a laser scanning confocal microscope (Zeiss LSM710).

2.17 2D Imaging of Tissue Cuts

Brightfield images of trichrome stained samples were taken with epifluorescence microscope (Zeiss AxioImager2) and high-resolution fluorescent images were taken with a confocal microscope (Zeiss LSM710). Image acquisition and optimization brightness and contrast was adjusted.

2.18 Image analysis and Statistics

Images were processed and analyzed with ImageJ (version 2.1.0). Statistical analyses were performed using GraphPad Prism software (v.9.4.1). Statistical significance was assessed by ONE-Way ANOVA to compare 3 groups.

3. Results

First, an optimal 4-OH tamoxifen concentration was established in order to enable single cell labeling of mesothelial cells on the surfaces of organs Single cell analysis would help us to investigate the clonal expansions emerging from the labelled single cells over time. For this, new double transgenic mice were created using ProcrCreER and PDPNCreER, both of which label the mesothelial lining of organ surfaces. The optimal 4-OH tamoxifen concentration was established as 2mg per injection, and for adult PDPNCreER mice it was established as 1 mg per injection. For newborn (ProcrCreER, and PDPNCreER), this dropped to 0.125mg per injection (data not shown). After the determination of optimal 4-OH tamoxifen concentration for single cell recording, organ surfaces were determined to compare Procr and PDPN positive mesothelial cells. Procr and PDPN positive cells showed similar phenotype when compared to each other for all the collected organs. Then, as the second proof these organs were stained for PDPN protein as a cell surface marker, both Procr and PDPN positive mesothelial cells showed the co-localization with the surface marker.

3.1 Healthy mesothelium clonality change

3.1.1 Adult mesothelium clonality change – young to aged

Under homeostatic condition, it has been shown in an *in vitro* study that the proliferation rate of adult mesothelium is estimated between 0.16-0.5% of total cells. (Steven E. Mutsaers, 2002). To determine the *in vivo* proliferation capacity of mesothelial cells during homeostasis, tamoxifen treatment and recombination was induced in PDPNCreER **(Figure 10A)** and in ProcrCreER **(Figure 11A)** transgenic mouse models under the TM4 reporter system ($R26^{mTmG}$) **(Figure 10A,11A).** For this, mice were injected with 4-hydrotamoxifen (4-OH Tam) via i.p. route one time at the age of 6-7 weeks (Methods). Our first goal was to label single mesothelial cells on the surface of organs. This approach later helped us to observe the behaviour of single mesothelial cells and study their clonality during the cumulative year. After 7 days, it was observed that only single mesothelial cells turned into green and indicating recombination had occurred in single cells

(Figure 10B, 11B). After the confirmation of single cell labelling of surface mesothelium, the remaining mice were injected with the optimal concentration of 4-OH Tam and left in the animal house for long-term cell tracing studies (1 year). Samples were collected after 3 months, 6 months and 1 year **(Figure 10A, 11A)**. Surface images of organs were taken under the confocal microscope **(Figure 10B,11B).** Clusters or clones of mesothelial cells were defined as 1, 2, 3, 4 cell clones and clones containing more than 5 cells were defined in the category of >5 cell clone **(Figure 10D,11D).** Clonality changed throughout the year in different organs were defined as percentage (dividing total clone numbers to total cell number). There was no drastic change between organs. Clones bigger than 15 cells were observed between organs as well as between two different transgenic mice **(Figure 10D,11D)**. Symmetric cell divisions in mesothelial cells were approximately 20%-40% higher than a-symmetric cell divisions **(Figure 10C,11C).**

ProcrCreER lineage traced peritoneum showed that, clones of 5 cells were significantly increasing when compared to 3 month and 6 months. However, PDPNCreER lineage traced peritoneum showed bigger than 5 cell clones were decreased when compared to 3 months and 6 months **(Figure 12a',12b').** Livers from ProcrCreER lineage traced mice did not have clone sizes bigger than 5 clones, on the other hand liver from PDPNCReER lineage traced mice had clone sizes bigger than 5 cells, but the change observed after a year was decreasing significantly **(Figure 12a'',12b'').** Caecum from ProcrCreER lineage traced mice did not have clone sizes bigger than 5 clones after a year, but caecum from PDPNCReER lineage traced mice had clone sizes bigger than 5 cells, the change determined after a year was significant **(Figure 12a''',12b''').** Same was found for lungs, where ProcrCreER lineage traced mice showed significance and PDPNCreER lineage traced mice did not show significance of clonal sizes bigger than 5 clones after a year **(Figure 12a'''',12b'''').** Heart mesothelium from ProcCReER and PDPNCreER lineage traced mice had no clones bigger than 5 cells after a year **(Figure 12a''''',12b''''').** We conclude that clonal dynamics is similar across both transgenic lines with absence of significant differences at 1 year of tracing **(Figure 12).**

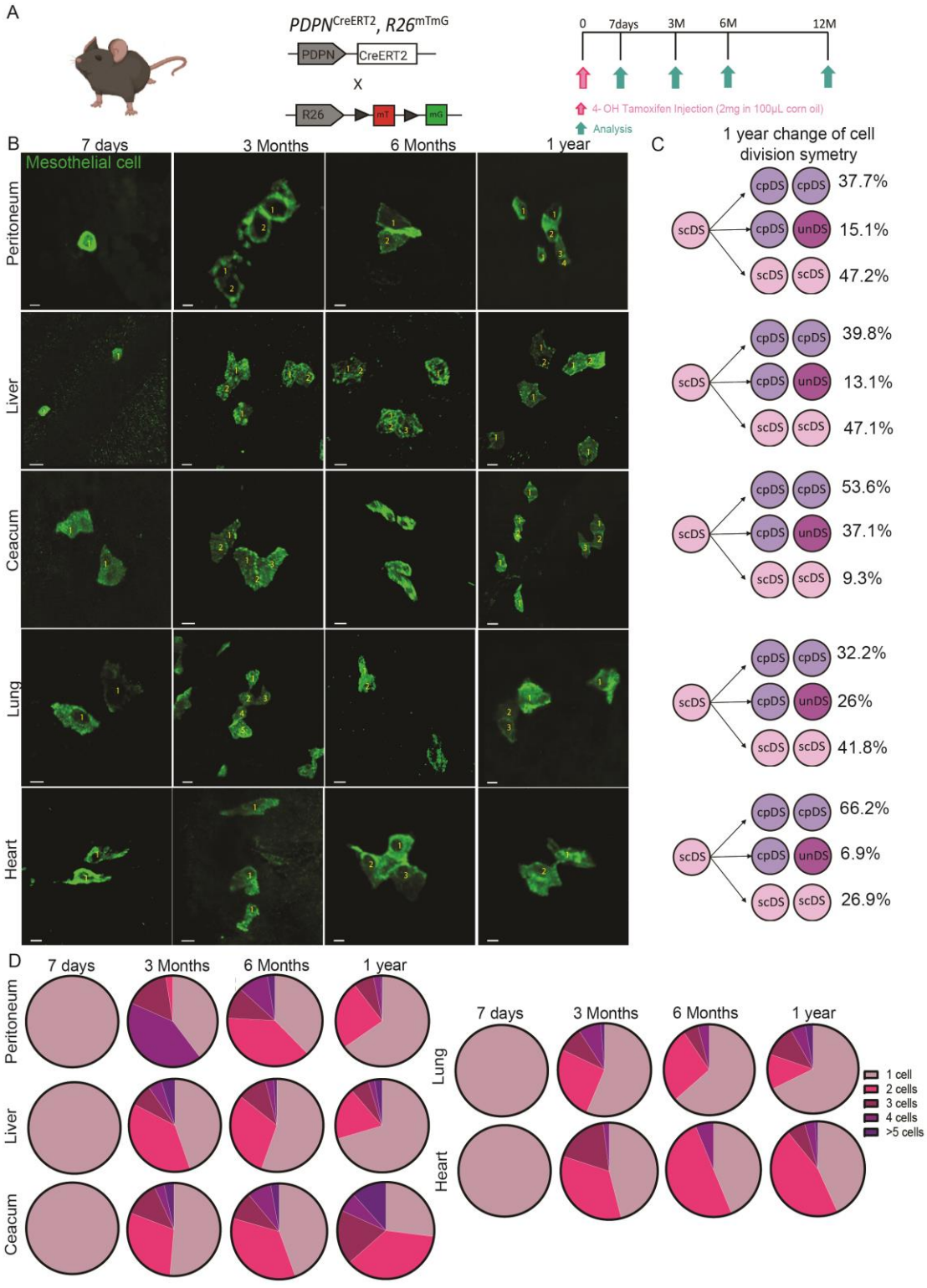

Figure 10: Adult mesothelial clonality data of PDPNCreER x TM4 transgenic mouse system. (A) Overview of experimental set up PDPNCreER x TM4 mouse for tamoxifen injection and organ collection time points. (B) Confocal images of clones after 7 days, 3, 6 months and 1 year. Organs collected were peritoneum, liver, ceacum, lung and heart. Scale bar 20um. (C) Cell division symmetry of mesothelial cell in total population of clones (cpDS-cpDS is symmetric division, cpDS-unDS is unsymmetric division) (D) Clonal changes from single cell to >5 cells for the above-mentioned time points.

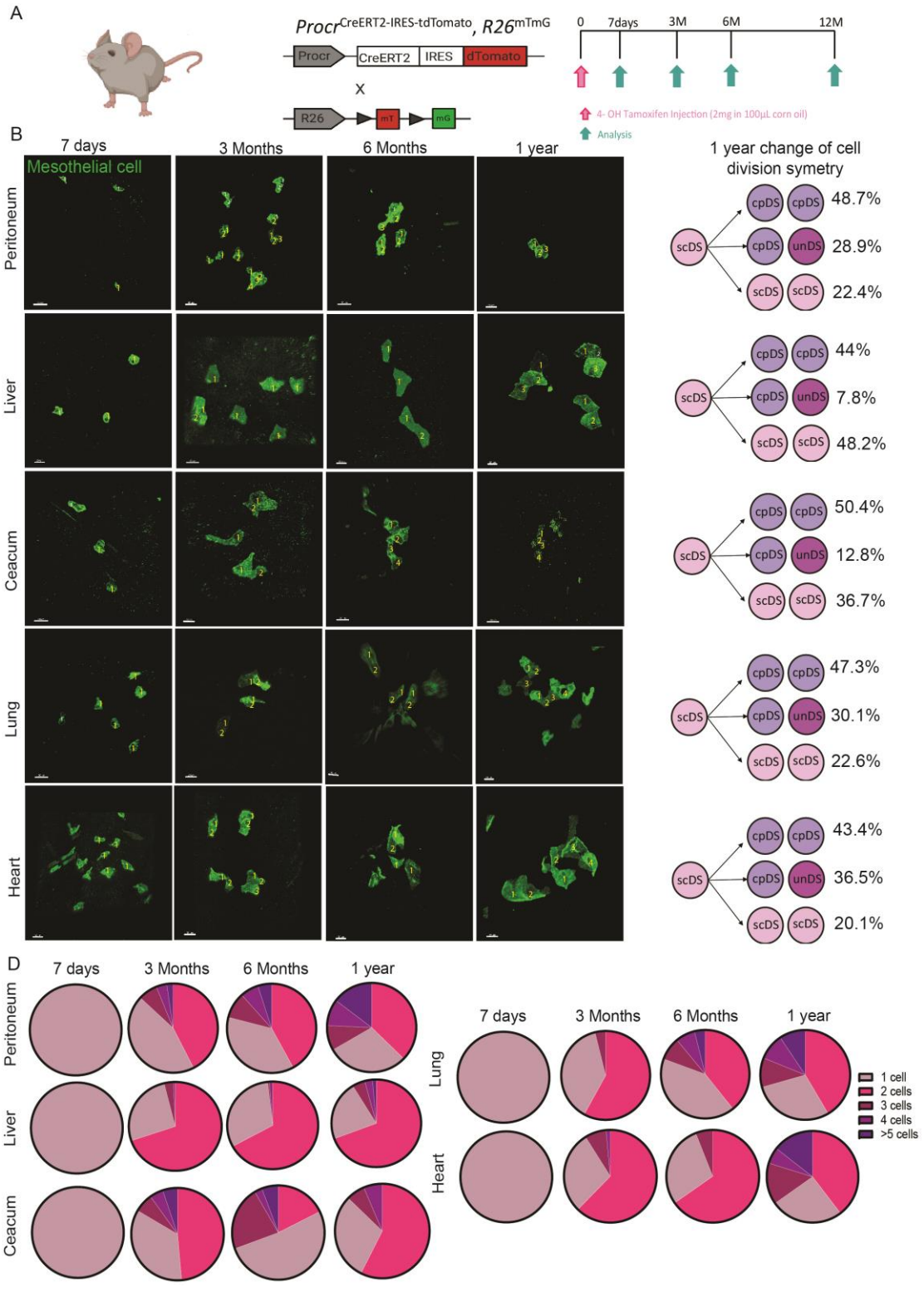

Figure 11: Adult mesothelial clonality data of ProcrCreER x TM4 transgenic mouse system. (A) Overview of experimental set up ProcrCreER x TM4 mouse for tamoxifen injection and organ collection time points. (B) Confocal images of clones after 7 days, 3 months, 6 months and 1 year. Organs collected were peritoneum, liver, ceacum, lung and heart. Scale bar 20um. (C) Cell division symmetry of mesothelial cell in total population of clones (cpDS-cpDS is symmetric division, cpDS-unDS is unsymmetric division) (D) Clonal changes from single cell to >5 cells for the above-mentioned time points.

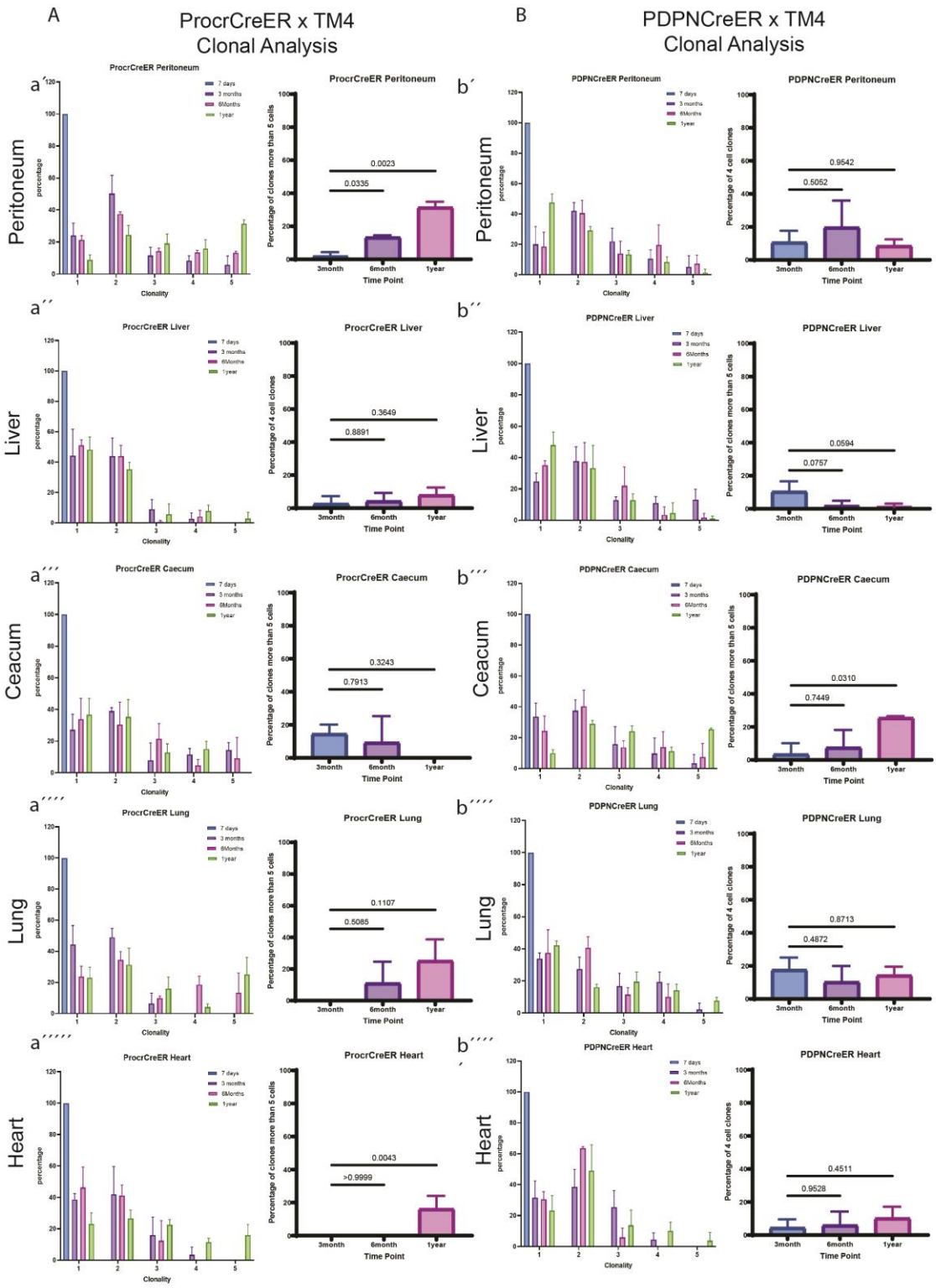

Figure 12: Adult mesothelial clonality. (A) Clonal percentage calculation of ProcrCreER x TM4 (a´) Peritoneum, 1 year p value < 0.05 (a``) Liver, 1 year p value > 0.05 (a´´´) Ceacum, 1 year p value > 0.05 (a´´´´) Lung, 1 year p value > 0.05 (a´´´´´) Heart, 1 year p value < 0.05. (B) Clonal percentage calculation of PDPNCreER x TM4 (b´) Peritoneum, 1 year p value > 0.05 (b``) Liver, 1 year p value < 0.05 (b´´´) Ceacum, 1 year p value < 0.05 (b´´´´) Lung, 1 year p value > 0.05 (b´´´´´) Heart , 1 year p value > 0.05

3.1.2 Mesothelial-to-mesenchymal (MMT) transition of adult mesothelium – young to aged

It is known that mesothelial cells undergo MMT during development (Koopmans & Rinkevich, 2018). Here, mesothelial cells were determined whether they undergo MMT throughout 1 year of tracing. For this, mesothelial cells were traced by using our 2 new reporter mouse systems, TM4 ($R26^{mTmG}$) under the mesothelial specific promoters, PDPN and Procr **(Figure 13,14).** Mice were injected with 4-OH tamoxifen, 3 times to label almost all the mesothelial cells on the surface of organs **(Figure 13A,14A**, see Methods section**).** Thereafter, the organs were collected and were cut into sections to investigate MMT and cell movement inside the organs. Alpha smooth muscle actin (α-SMA) was used as MMT/fibroblast marker. Mesothelial cells were observed on the surface of organs (peritoneum, caecum, liver, lung and heart) in both 7 day and 1-year samples **(Figure 13,14).** PDPN and Procr positive cells in peritoneum did not show any movement inside organs and did not show differentiation into fibroblasts over 1 year in healthy mice **(Figure 13B, 14B).** PDPN and Procr positive cells in liver did not show any movements inside organs and did not show differentiation over a year in healthy mice **(Figure 13C, 14C).** PDPN and Procr positive cells in caecum indeed showed movements of mesothelial cells below the basement membrane (sub-capsule area) but did not show differentiation and migration inwards over time **(Figure 13D, 14D).** PDPN and Procr positive cells in lungs did not show any movement inside organs and did not show differentiation over time **(Figure 13E, 14E).** PDPN and Procr positive cells in heart did not show any movement inside organ and did not show differentiation over time **(Figure 13F, 14F).** Over a year, the numbers of mesothelial cells labelled with 4-OH tamoxifen in the beginning on the organ surfaces were not changed as compared to day 1 post labelling **(Figure 13,14).** When histologic analysis was completed and compared across each organ for green cells (TM4+) which represents mesothelial cells, distribution of mesothelial cells from the original clones were also similar. When the behaviour of Procr mesothelial cells to PDPN positive cells were compared, they were similar too.

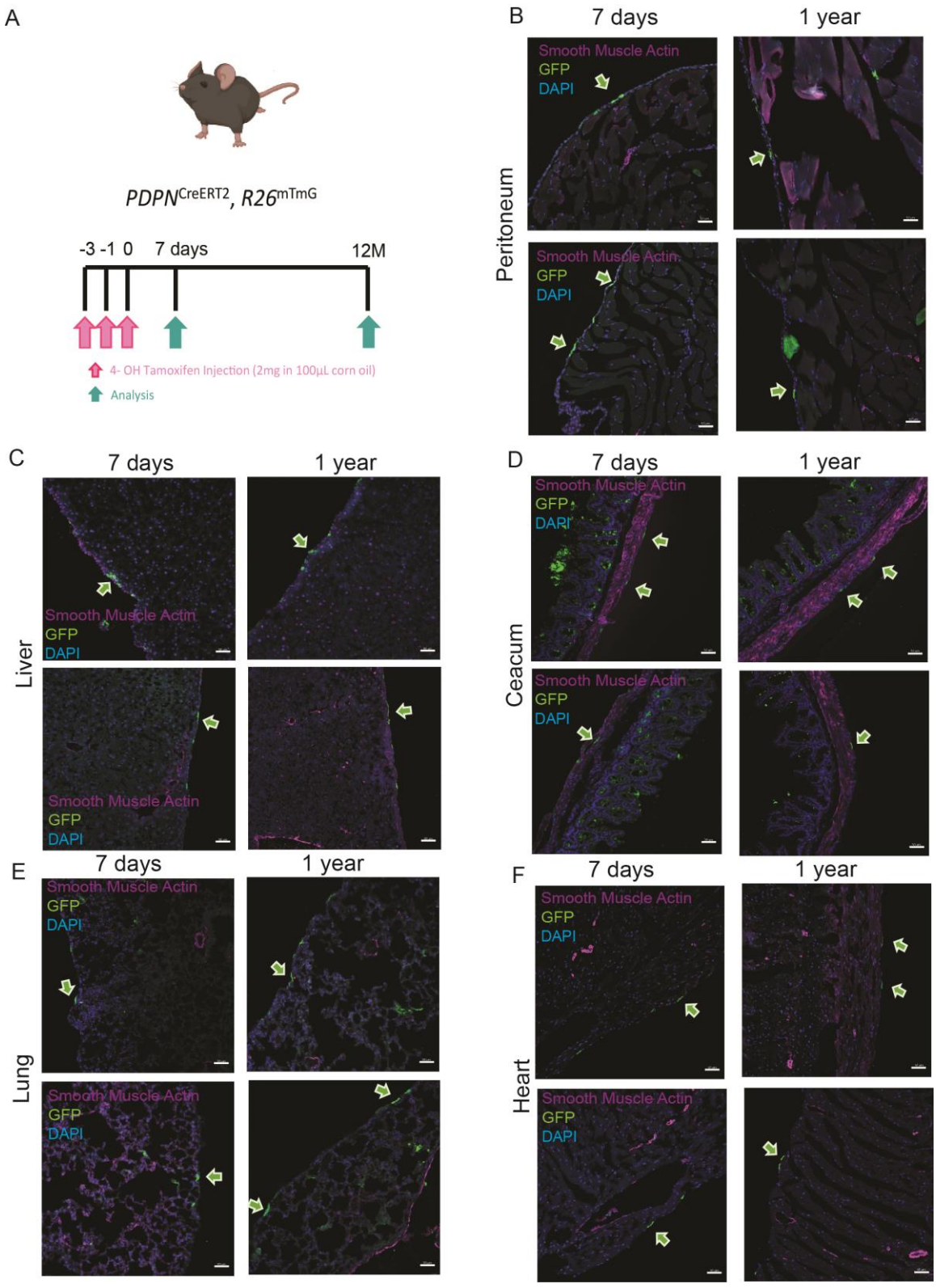

Figure 13: Adult mesothelial cell tracing data of PDPNxTM4 transgenic mouse system. (A) Overview of experimental set up PDPNCreER x TM4 mouse for tamoxifen injection and organ collection time points. Confocal images of organs such as peritoneum (B), liver (C), caecum (D), lung (E), heart (F) sections after 7 days, and 1 year. Scale bar 50 µm. (Green arrows were showing the traced mesothelial cells and magenta was showing the α-SMA staining, blue was DAPI).

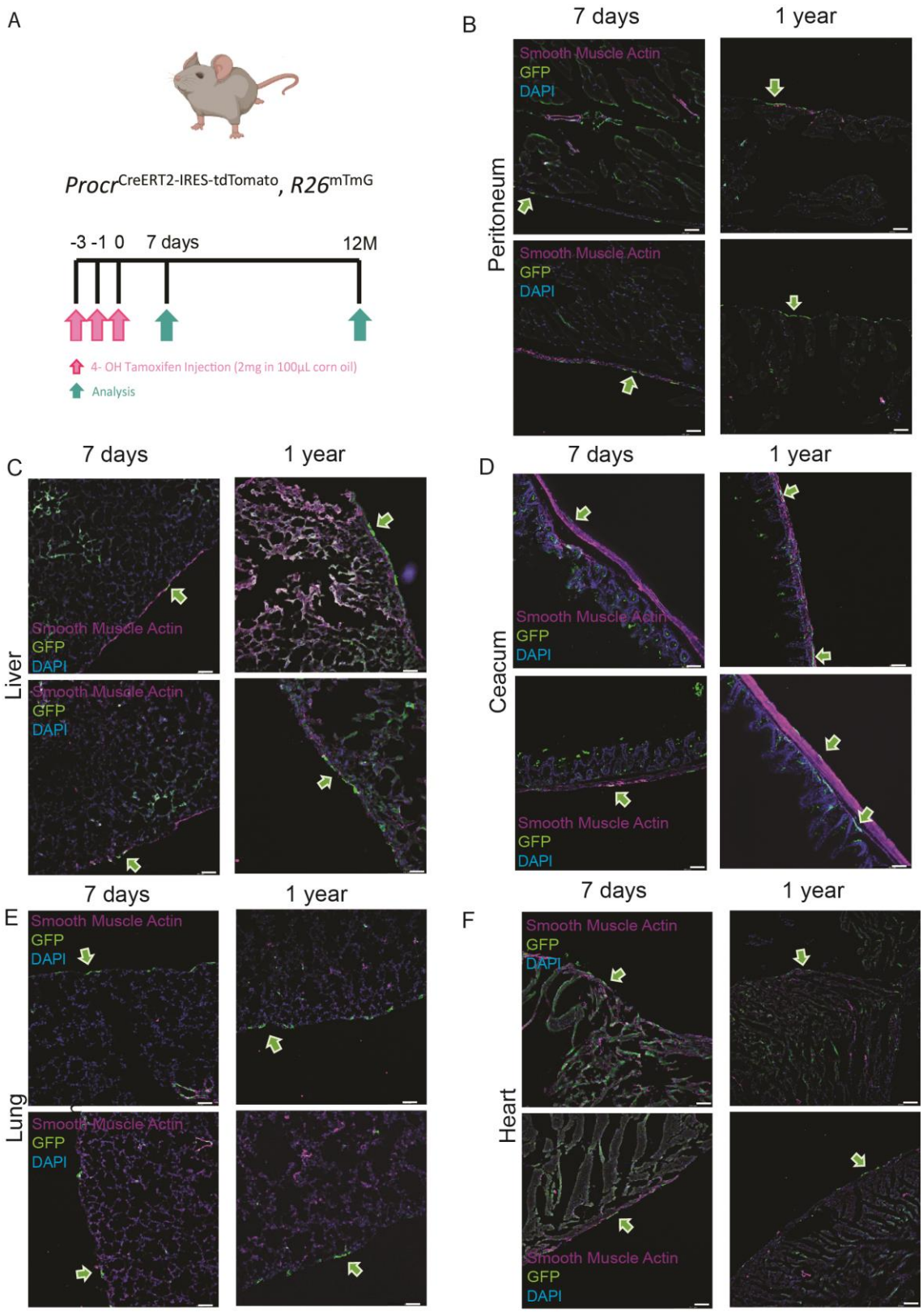

Figure 14: Adult mesothelial cell tracing data of ProcrCreERxTM4 transgenic mouse system. (A) Overview of experimental set up ProcrCreER x TM4 mouse for tamoxifen injection and organ collection time points. Confocal images of organs such as peritoneum (B), liver (C), caecum (D), lung (E), heart (F) sections after 7 days, and 1 year. Scale bar 50 µm. (Green arrows were showing the traced mesothelial cells and magenta was showing the α-SMA staining, blue was DAPI).

3.2 Clonal analysis of mesothelium during development

During developmental stages, mesothelial cells are highly proliferative and differentiation rates of mesothelial cells is high (Koopmans & Rinkevich, 2018). Organ growth and development continues after birth until the adult stage (6-7 weeks old mouse). Mesothelial cell clonality changes were investigated during postnatal development. Same two transgenic mouse models specific to mesothelium were used, PDPNCreER **(Figure 15A)** and ProcrCreER **(Figure 16A)**. Mesothelial cell clonality was traced by using same reporter mice, TM4 ($R26^{mTmG}$) under the mesothelial specific promoters, PDPN and Procr **(Figure 15A,16A).** 4-hydrotamoxifen (4-OH Tam) was injected via i.p. route once into new born P0 mice. 2 days after the first injection samples were collected and clonality of surface mesothelium was analyzed. An increase in mesothelial clonality after 2 days was observed. Clonal average and clonal maximum (7 cells clones) were similar to 1-year clonality change across many organs in adults under homeostasis **(Figure 15B, 16B).** After 7 days, clonality continued to increase and after 30 days clonality reached its peak. Single clone numbers in different organs reached approximately 30 cells per clone (Data not shown). Representative surface organ images were taken using a confocal microscope and changes in clonality were shown in Figure 15B and 16B for both PDPN and Procr positive mesothelial cells. To make the calculation easier and comparable to healthy adult stages, clones bigger than 5 cells were combined in one category and approximate change was visualized in pie charts. Clonality in both PDPN and Procr positive mesothelial cells in all organs increased drastically (60 cell clones in the heart, 50 cells clone in the lung, 38 cell clones in the peritoneum and 26 cell clones in the liver) (**Figure 15D,16D).** I was also interested in the cell division symmetry during postnatal development. Cell division symmetry were ordinally asymmetric and symmetric **(Figure 15C,16C).** When PDPN and Procr positive mesothelial cells were compared, it observed that they show the same phenotype.

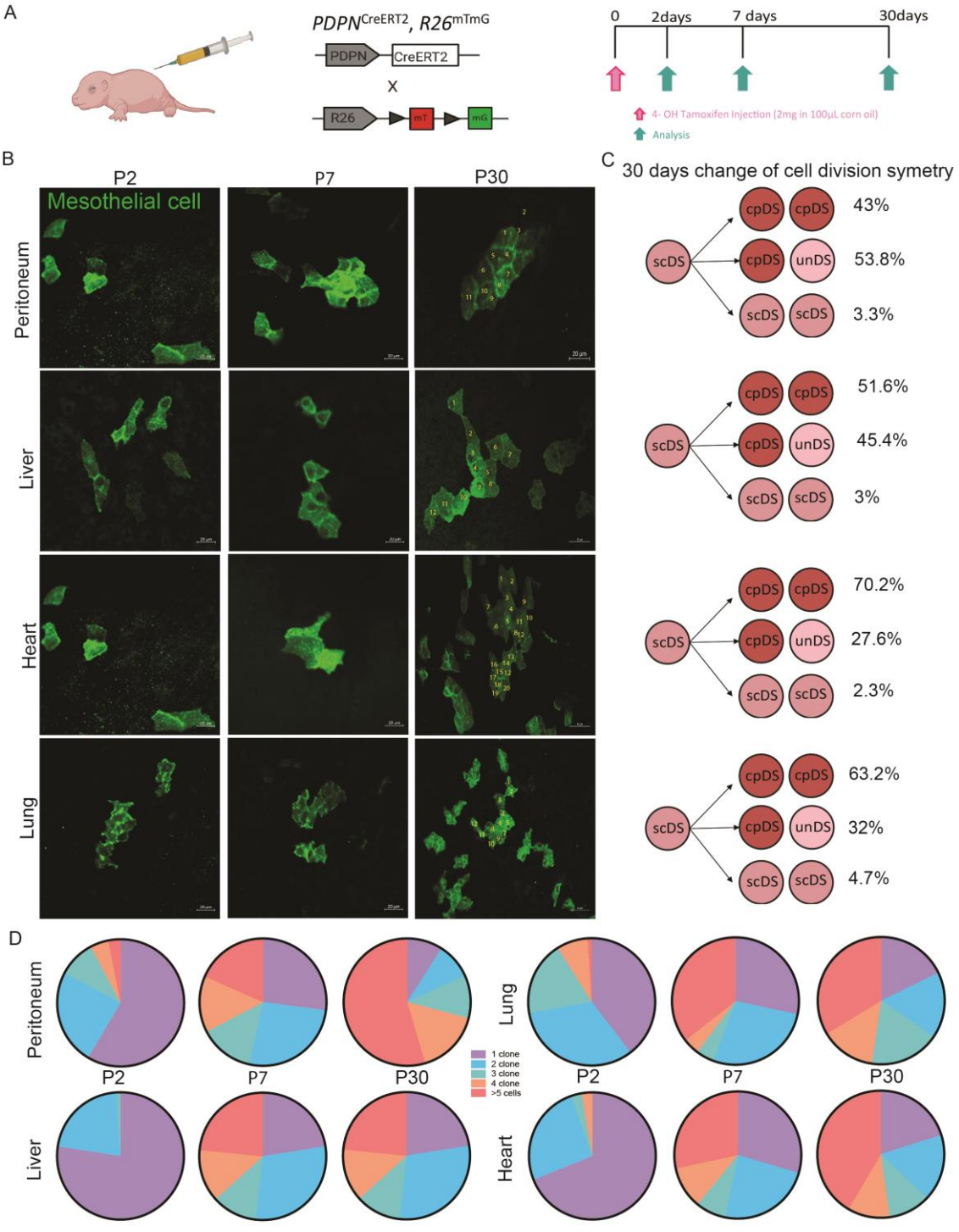

Figure 15: Neonatal mesothelial clonality data of PDPNCreER x TM4 transgenic mouse system. (A) Overview of experimental set up PDPNCreER x TM4 mouse for tamoxifen injection and organ collection time points. (B) Confocal images of clones after 2-, 7-, 30- days birth. Organs collected were peritoneum, liver, lung and heart. Scale bar 20 µm and 50 µm. (C) Cell division symmetry of mesothelial cell in total population of clones (cpDS-cpDS is symmetric division, cpDS-unDS is unsymmetric division) (D) Clonal changes from single cell to >5 cells for the above mentioned timepoints.

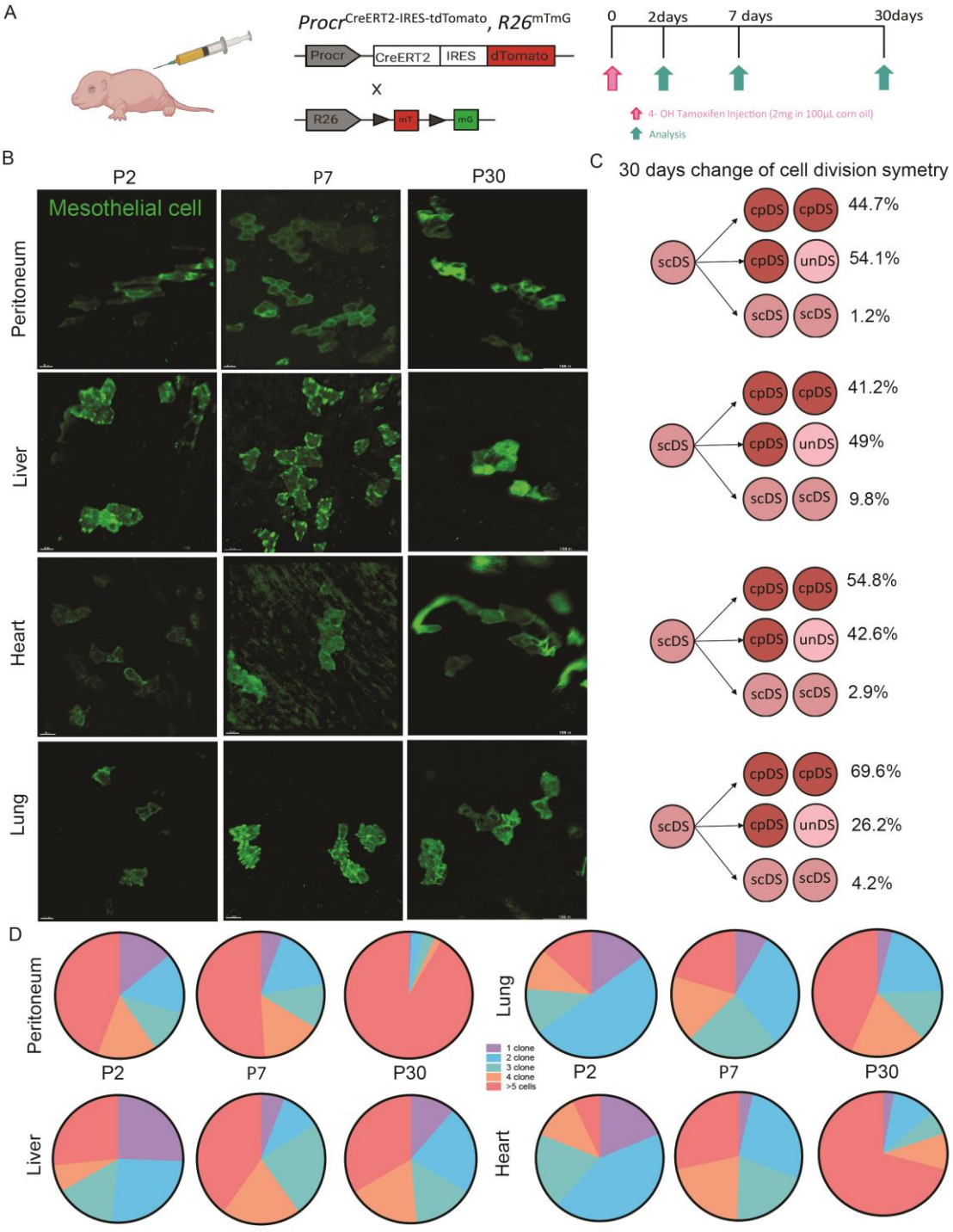

Figure 16: Neonatal mesothelial clonality data of ProcrCreER x TM4 transgenic mouse system. (A) Overview of experimental set up ProcrCreER x TM4 mouse for tamoxifen injection and organ collection time points. (B) Confocal images of clones after 2-, 7-, 30- days birth. Organs collected were peritoneum, liver, lung and heart. Scale bar 20 µm and 50 µm. (C) Cell division symmetry of mesothelial cell in total population of clones (cpDS-cpDS is symmetric division, cpDS-unDS is unsymmetric division) (D) Clonal changes from single cell to >5 cells for the above mentioned timepoints.

In figure 17, clonality changes during postnatal development were analysed for both Procr and PDPN. Procr and PDPN peritoneum **(Figure 17a',17b')** and heart **(Figure 17a'''',17b'''')** showed a statistical increase in clones bigger than 5 cells as compared to 2 days. In addition, Procr liver **(Figure 17a'',17b'')** and lung **(Figure 17a''',17b''')** also showed an increase in clone size bigger than 5 cells but failed to reach statistical significance. PDPN liver **(Figure 17a'',16b'')** and lung **(Figure 17a''',17b''')** showed a statistically significant increase in clones bigger than 5 cells in comparison to 2 days.

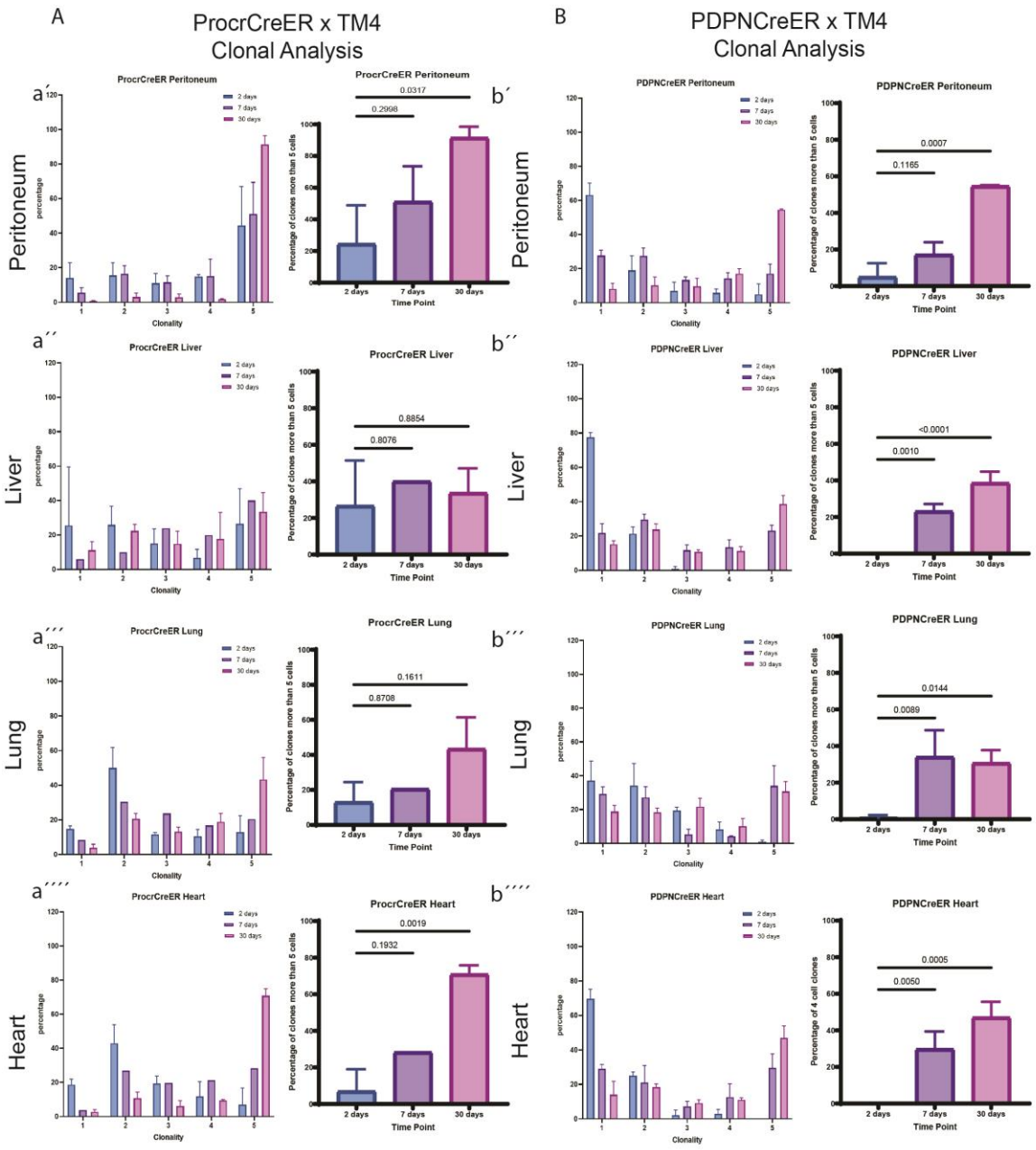

Figure 17: Neonatal mesothelial clonality. (A) Clonal percentage calculation of ProcrCreER x TM4 (a´) Peritoneum, 30 days p value < 0.05 (a``) Liver, 30 days p value > 0.05 (a´´´) Lung, 30 days p value > 0.05 (a´´´´) Heart, 30 days p value < 0.05. (B) Clonal percentage calculation of PDPNCreER x TM4 (b´) Peritoneum, 30 days p value < 0.05 (b``) Liver, 30 days p value < 0.05 (b´´´) Lung, 30 days p value < 0.05 (b´´´´) Heart, 30 days p value < 0.05

3.3 Clonality change of mesothelium under injury conditions

Under injury conditions, mesothelial cells undergo activation (Steven E. Mutsaers, 2004). I investigated the clonality changes in mesothelial cells under a variety of acute and chronic injury conditions.

3.3.1 Abdominal fibrosis by surgical adhesions

Our previously described 2 lineage tracing systems were used to study clonality in mesothelium during postsurgical adhesions. Previous studies by our group have shown that post-surgical adhesions occur from mesothelial cells, but not from matrix depositing fibroblasts (Figure 5) (Rinkevich et al., 2014; Tsai et al., 2017). In addition, mesothelial cells were depleted by using the transgenic mouse model, and observed to be absent of adhesions when the lining mesothelial cells are removed **(Figure 6)** (Fischer et al., 2020)

Abdominal fibrosis was induced by surgical adhesions between caecum and peritoneum. Mesothelial cell clonality under injury conditions were traced by using reporter mice, Ai14 under the mesothelial specific promoters, PDPN and Procr, as before **(Figure 18A,19A).** Adhesions fully appeared between caecum and peritoneum after 5 days of post-surgery **(Figure 18B, 19B).** Red arrows in the figure 18B and 19B show the connection points between caecum and peritoneum. I also observed in few instances that the adhesions were observed between peritoneum and liver **(Figure 18B).** After 5 days of post-surgery on the injured peritoneum, many red-labelled mesothelial cells were observed **(Figure 18C,19C)** and clonality of these cell clusters was drastically higher than adult mesothelium after 1 year **(Figure 10,11).** Adhesion samples were cut for histological analysis and surface imaging. Histological analysis of injured peritoneum showed thickening at the adhesion area **(Figure 18D,19D).** Proliferation assay with Ki67 staining was performed to show the mesothelial cell proliferation during injury. I observed co-localization between mesothelial cells (in red) with Ki67 (in green) **(Figure 18E,19E).** In our histological cuts, I also observed movement of mesothelial cells inside the peritoneum **(Figure 18E,19E).**

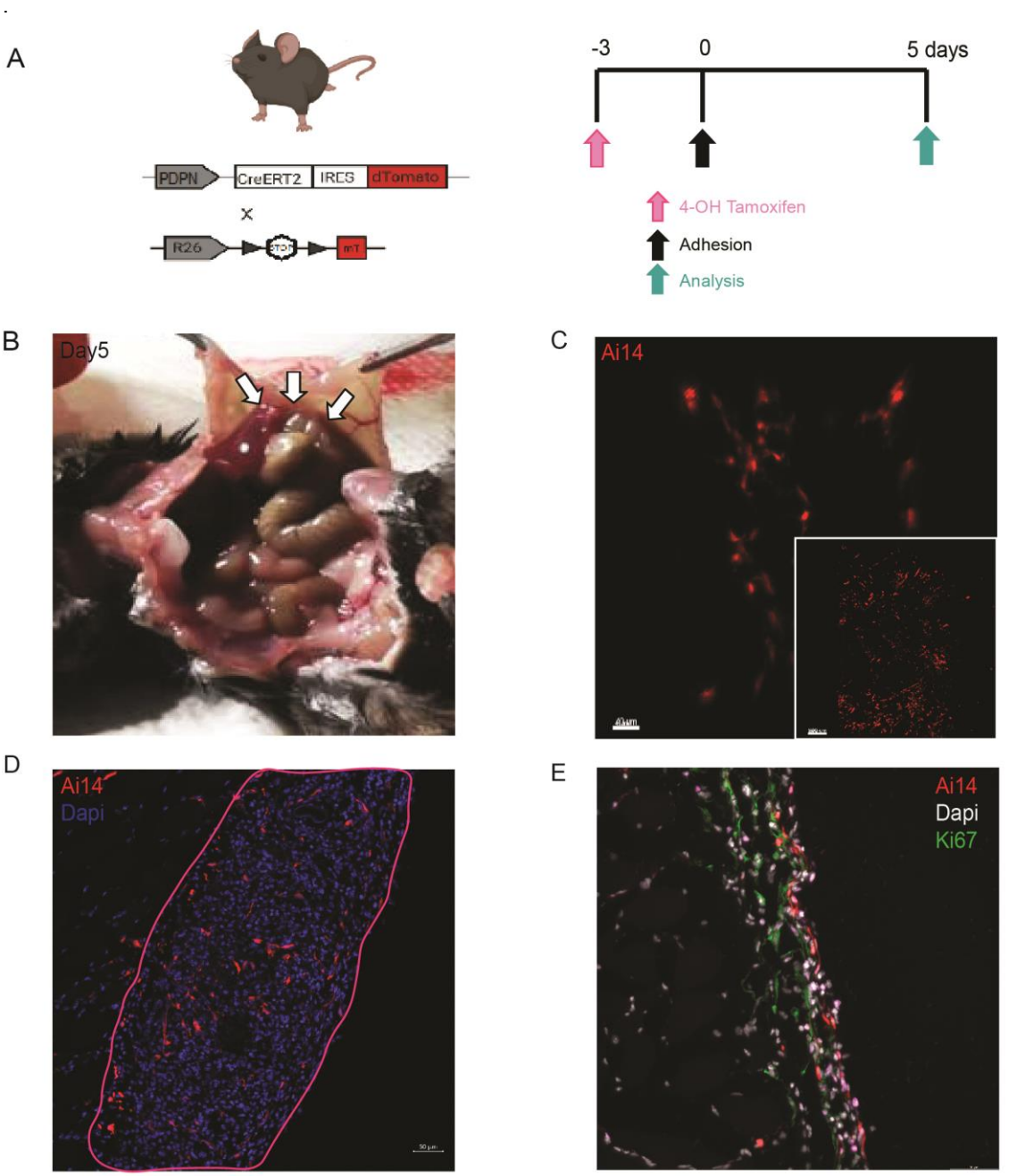

Figure 18: Clonality change during abdominal adhesions of PDPNCreER x Ai14. (A) Overview of experimental set up PDPNCreER x Ai14 mouse for tamoxifen injection, induction of injury and the time point for organ collection. (B) Adhesion between caecum and peritoneum post-surgery. (C) Surface confocal image of injured peritoneum. Scale bar 40µm and 300µm. (D) Histological cut of injured peritoneum. Red cells represent the mesothelial cells and blue cells represent DAPI staining. Scale bar 50um. (E) Cell proliferation staining of injured peritoneum. Green cells represent Ki67 staining, red cells represent the mesothelial cells and white cells represent DAPI staining. Scale bar 50µm.

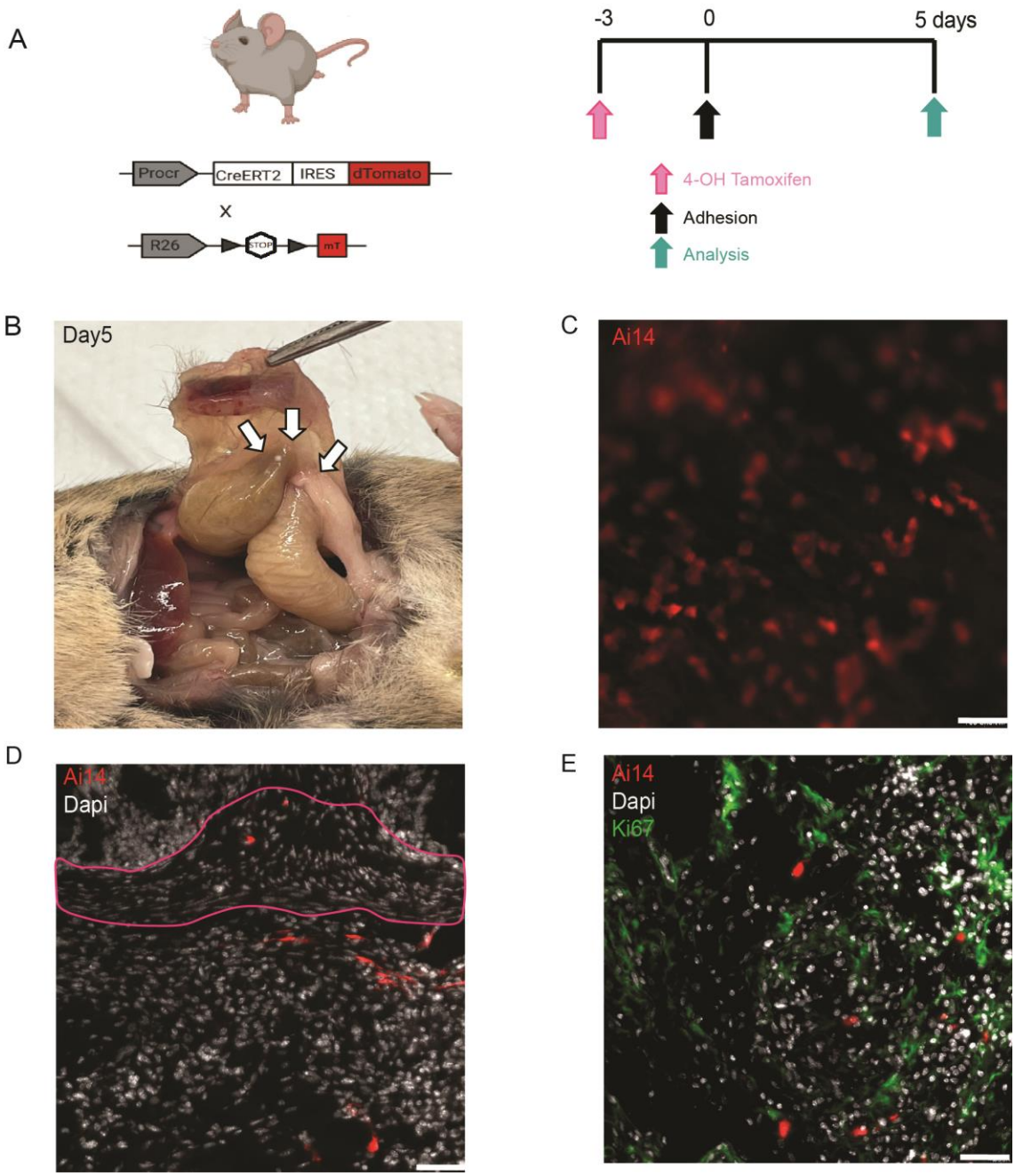

Figure 19: Clonality change during abdominal adhesions of ProcrCreER x Ai14. (A) Overview of experimental set up ProcrCreER x Ai14 mouse for tamoxifen injection, induction of injury and the time point for organ collection. (B) Adhesion between caecum and peritoneum post-surgery. (C) Surface confocal image of injured peritoneum. Scale bar 50µm. (D) Histological cut of injured peritoneum. Red cells represent the mesothelial cells and blue cells represent DAPI staining. Scale bar 50µm. (E) Cell proliferation staining of injured peritoneum. Green cells represent Ki67 staining, red cells represent the mesothelial cells and white cells represent DAPI staining. Scale bar 50µm.

3.3.2 Lung inflammation and fibrosis

Lung fibrosis was induced by Bleomycin intratracheal installation. Mesothelial cell clonality under injury were traced using reporter mice, Ai14 under the mesothelial specific promoters Procr as before **(Figure 20A).**

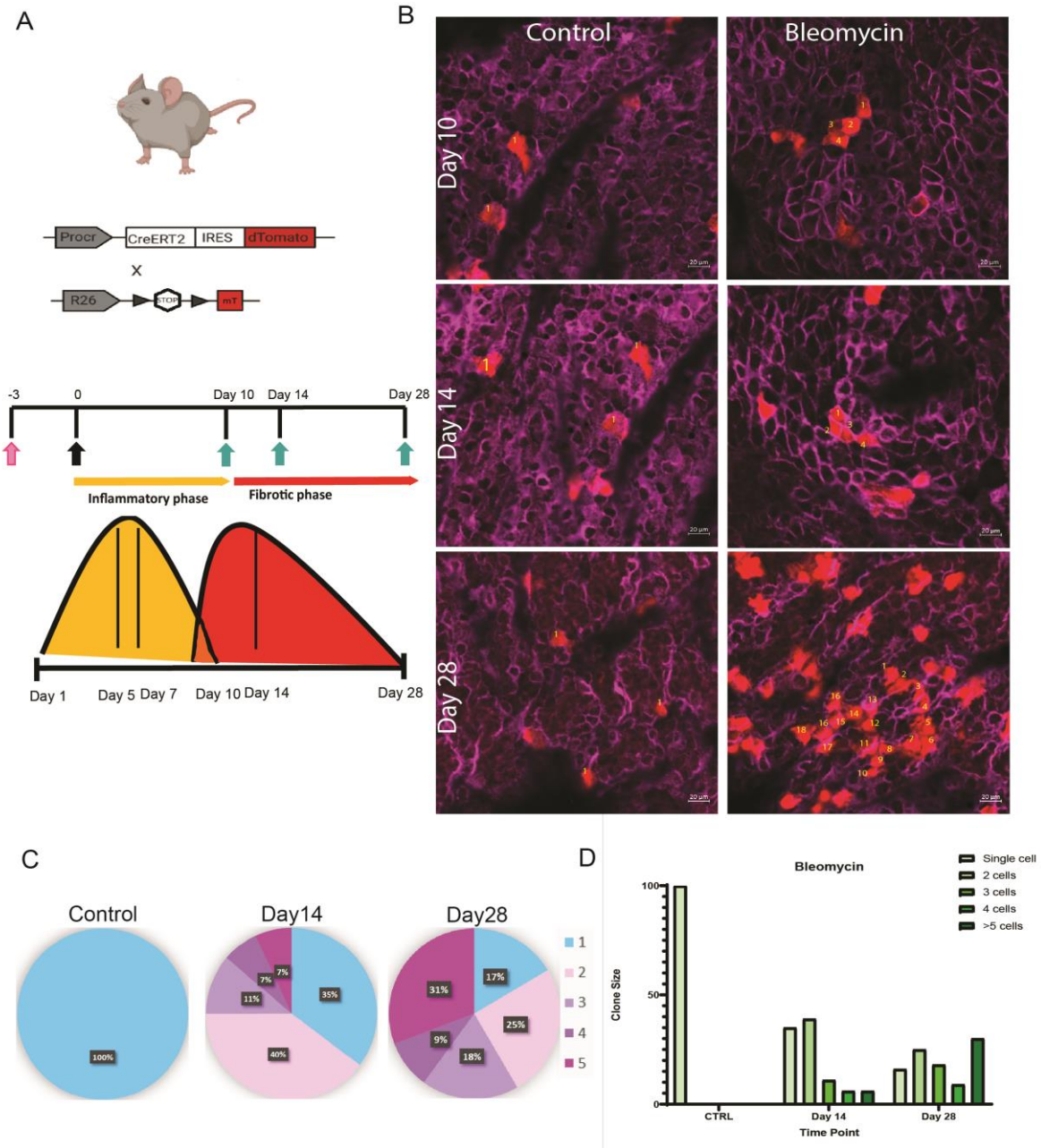

Figure 20: Clonality change during lung fibrosis of ProcrCreER x Ai14. (A) Overview of experimental set up ProcrCreER x Ai14 mouse for tamoxifen injection, induction of injury and the time points for organ collection. Different phases of lung injury, inflammatory phase to fibrotic phase is shown in the graph. (B) Surface confocal image of injured lung compared to control lung at day 10, 14 and 28. Magenta represents PDPN staining and red cells represent surface mesothelial cells. Scale bar 20µm. (C) Pie chart of clonality change during fibrosis. (D) Clonality change during lung fibrosis.

After bleomycin installation, the first 10 days accounts for the inflammation phase, and day 14 was the peak of the fibrotic phase. Whereas day 28 showed a gradual resolution of fibrosis **(Figure 20A).** Clonal counting at day 10 did not show a significant change when compared to controls. However, starting from day 14 clonality increased up to 18 cells per clone at day 28 post injury **(Figure 20B, C, D).**

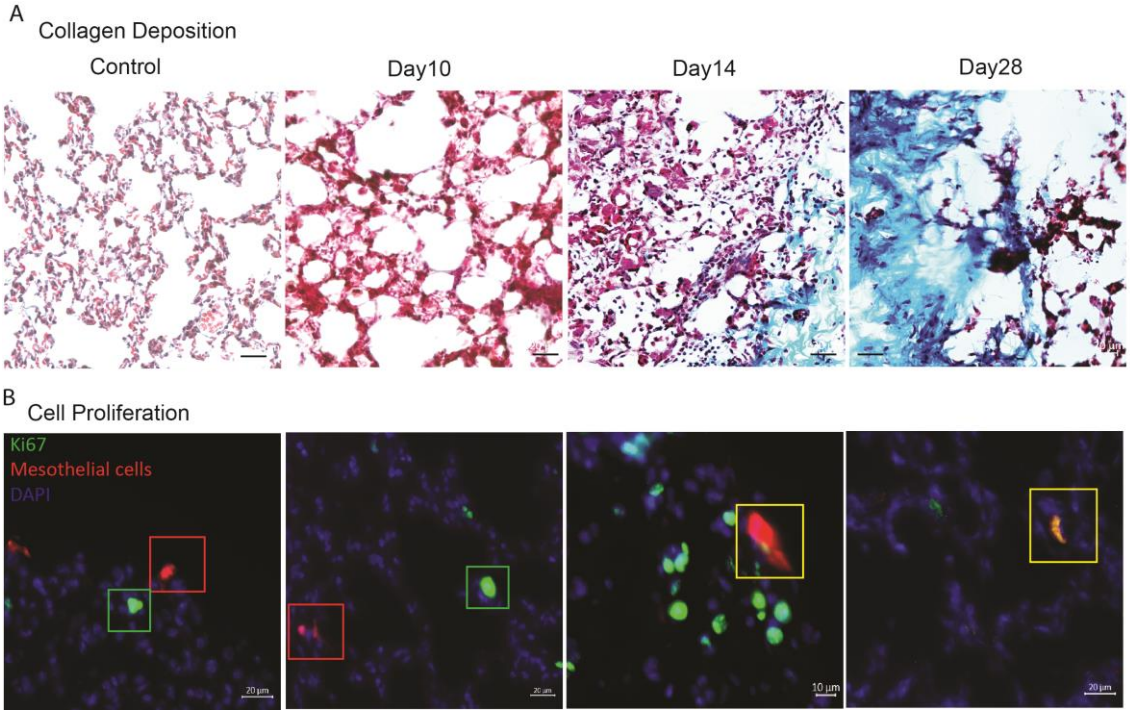

Figure 21: Histology of lungs after lung fibrosis. (A) Collagen deposition after day 10, 14 and 28 of injury. Cells are in black, collagens are in blue, muscles are in red and cytoplasm in pink. Scale bar 20µm. (B) Cell proliferation of mesothelial cells after day 10, 14 and 28 of injury. Cell proliferation marker Ki67 is in green, mesothelial cells are in red and DAPI is in blue. Scale bar 10µm and 20µm.

Trichrome staining was performed to show collagen deposition during fibrosis formation. Control and day 10 samples did not show collagen deposition, however collagen deposition started after day 14 and continued until day 28 **(Figure 21A).** Cell proliferation assay with Ki67 was performed to determine the mesothelial cell proliferative capacity. Mesothelial cells were co-localized with Ki67 at day 14 and day 28 (at the fibrotic phase), but not in the control and day 10 **(Figure 21B).**

3.3.3 Abdominal inflammation by LPS infection

Abdominal inflammation was induced by LPS infection. Mesothelial cell clonality under injury conditions were traced by using reporter mice, TM4 ($R26^{mTmG}$) under the mesothelial specific promoter, PDPN as before **(Figure 22A).**

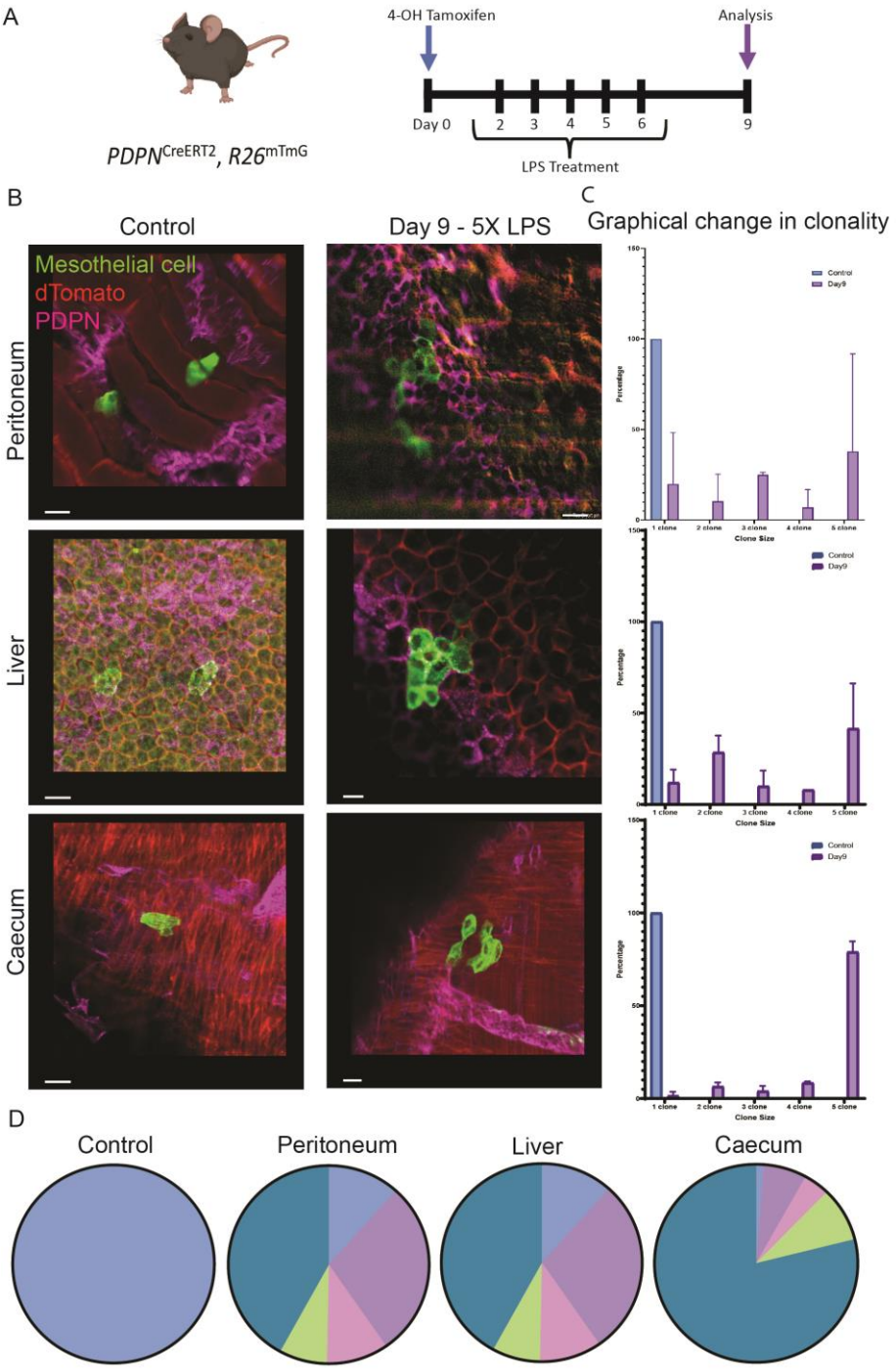

Figure 22: Clonality change during abdominal inflammation of PDPNCreER x TM4. (A) Overview of experimental set up PDPNCreER x TM4 mouse for tamoxifen injection, induction of injury and the time points for organ collection. (B) Surface confocal image of injured peritoneum, liver and caecum compared to control lung at day 9. Magenta represents PDPN staining and green cells represent surface mesothelial cells. Scale bar 20µm and 50µm. (C) Clonality change during abdominal inflammation. (D) Pie chart of clonality change during abdominal inflammation.

Surface of peritoneum, liver and caecum were imaged under the confocal microscope **(Figure 22B).** After 9 days of consecutive injection of LPS mesothelial cell clonality increased drastically in peritoneum, liver, and caecum when it compared to control **(Figure 23C, D).**

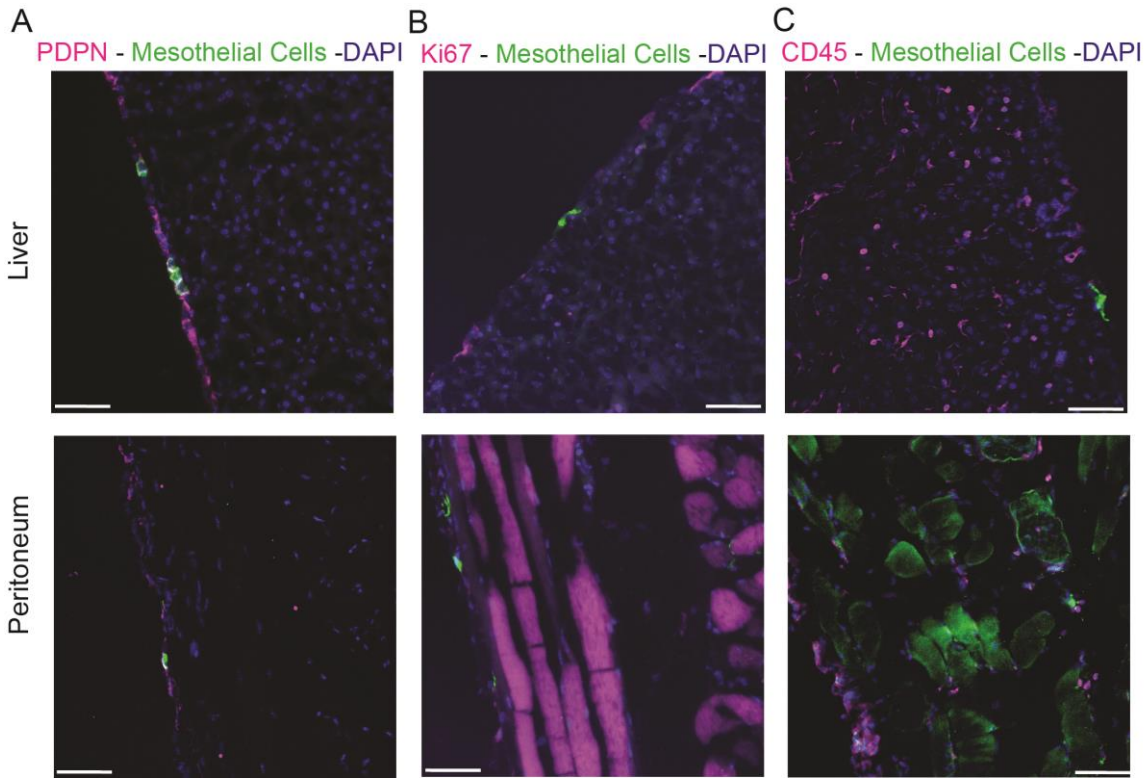

Figure 23: Histology of liver and peritoneum after abdominal inflammation. (A) Surface mesothelial staining with PDPN in magenta, mesothelial cells in green, DAPI in blue. (B) Cell proliferation marker in magenta, mesothelial cells in green, DAPI in blue. (D) Macrophage marker in magenta, mesothelial cells in green, DAPI in blue. Scale bars 50µm.

Histological cuts of liver and peritoneum were analyzed for cell proliferation. Macrophage cell numbers was also used as a read-out of inflammation. PDPN (in magenta) staining co-localized with mesothelial cells (in green) **(Figure 23A).** Co-localization of cell proliferation marker Ki67 (in magenta) was observed within mesothelial clones (in green) **(Figure 23B).** Macrophage cells (in magenta) was observed at the injury site but outside of the PDPN clone cluster. **(Figure 23C).**

3.4 Role of basement membranes in mesothelial clonality

Mesothelial cells attach and lay atop a basement membrane structure (Pozzi et al., 2017; Zheng & Yamada, 2019). Therefore, to understand the role of basement membranes in clonality, we first looked at lung fibrosis models **(Figure 24A).** I observed that CD54 (ICAM1, cell-cell interaction marker) increased in mesothelial cells at the peak of lung fibrosis (Day 14) and CD29 (ITGB1, cell-matrix interaction marker) increased in mesothelial cells at the end of the inflammation phase, and at the beginning of fibrosis phase (Day10). In additional organs such as liver and peritoneum, the expression of ICAM1 decreased in injured liver and peritoneum, but expression of ITGB1 was found to be increased **(Figure 24B).**

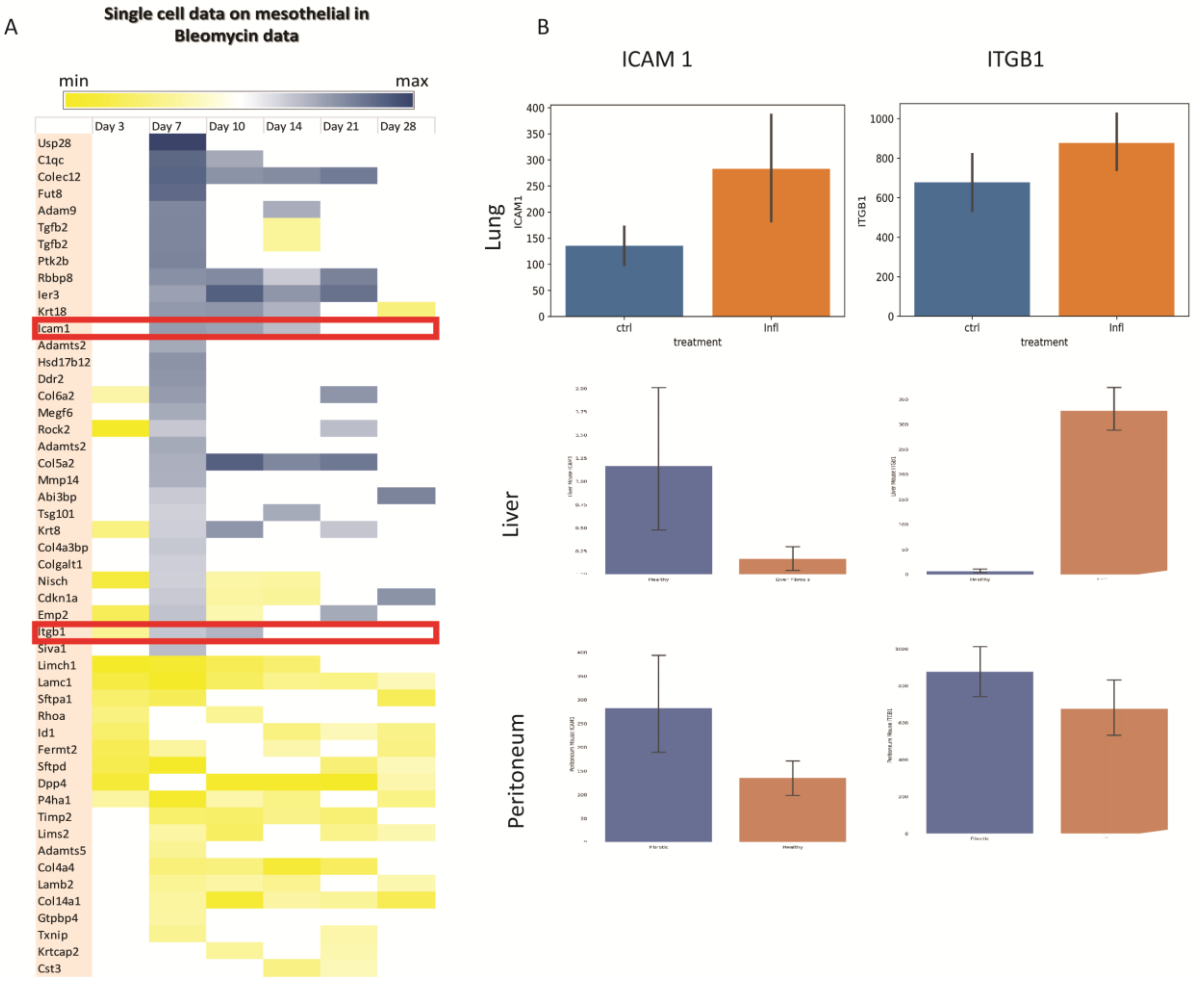

Figure 24: Single cell data of mesothelial cells during different injuries in various organs. (A) Expression of basement membrane molecules during lung fibrosis. Red box shows the ICAM1 and ITGB1. (B) ICAM1 and ITGB1 expression change during lung, liver, and peritoneum under stressed conditions compared to healthy lung, liver, and peritoneum.

3.4.1 Inhibiting CD29 and CD54 affects mesothelial clonality during development

Role of the basement membrane in clonality during postnatal development was investigated via blocking the CD29 and CD54 after birth in PDPNCreER x TM4 double transgenic mice ($R26^{mTmG}$) **(Figure 25A).** CD54 inhibition increased mesothelial clonality (68 cell clones in the liver, 32 cell clones in the peritoneum). Whereas CD29 inhibition led to the opposite effect with a decrease in cell clonality **(Figure 25B).**

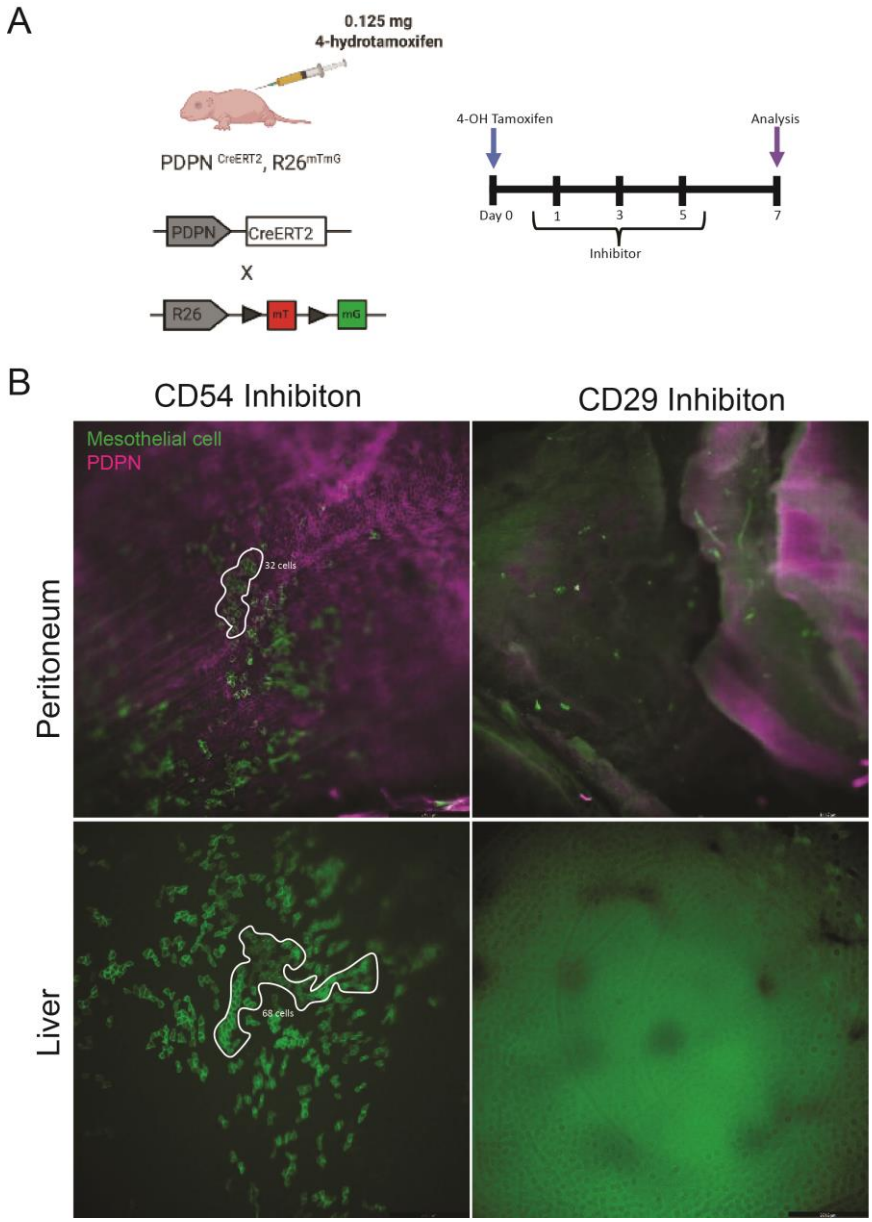

Figure 25: Post-natal development under the inhibition of basement membrane molecules of PDPNCreER x TM4. (A) Experimental set up. (B) Surface images with light microscope of peritoneum and liver after 7 days. Scale bars, Peritoneum left to right, 265.7µm, 841.7µm, Liver left to right 209.2µm, 209.2µm

3.4.2 Inhibiting CD29 and CD53 affects mesothelial clonality during injury

Role of the basement membrane in clonality during injury was investigated via blocking the CD54 and CD29 in PDPNCreER x Ai14 and ProcrCreER x Ai14 double transgenic mice **(Figure 26A).** At day 5 post-surgery, the adhesion between caecum and peritoneum connection sites were determined. Under CD54 inhibition, the connection between caecum and peritoneum, and the involvement of other organs in Procr mice were increased **(Figure 26B)** when compared to normal adhesions **(Figure 19A).** Under CD54 inhibition, the connection between caecum and peritoneum in PDPN mice also increased, but the involvement of other organs was not observed **(Figure 26B)** when compared to normal adhesions **(Figure 18A).** Thickening of the adhesion sites at the peritoneum was determined at the histological cuts. Thickening at the site of adhesion was larger in CD54 inhibited samples as compared to CD29 inhibited samples. When the samples were compared between Procr and PDPN, Procr mice showed more thickening than PDPN under the inhibition of CD54 **(Figure 26C).** Surface images of injured peritoneum were also determined under the inhibition of CD29 and CD54. Cell numbers in clones were higher under the inhibition of CD54 than CD29 in both Procr and PDPN mice **(Figure 26D).**

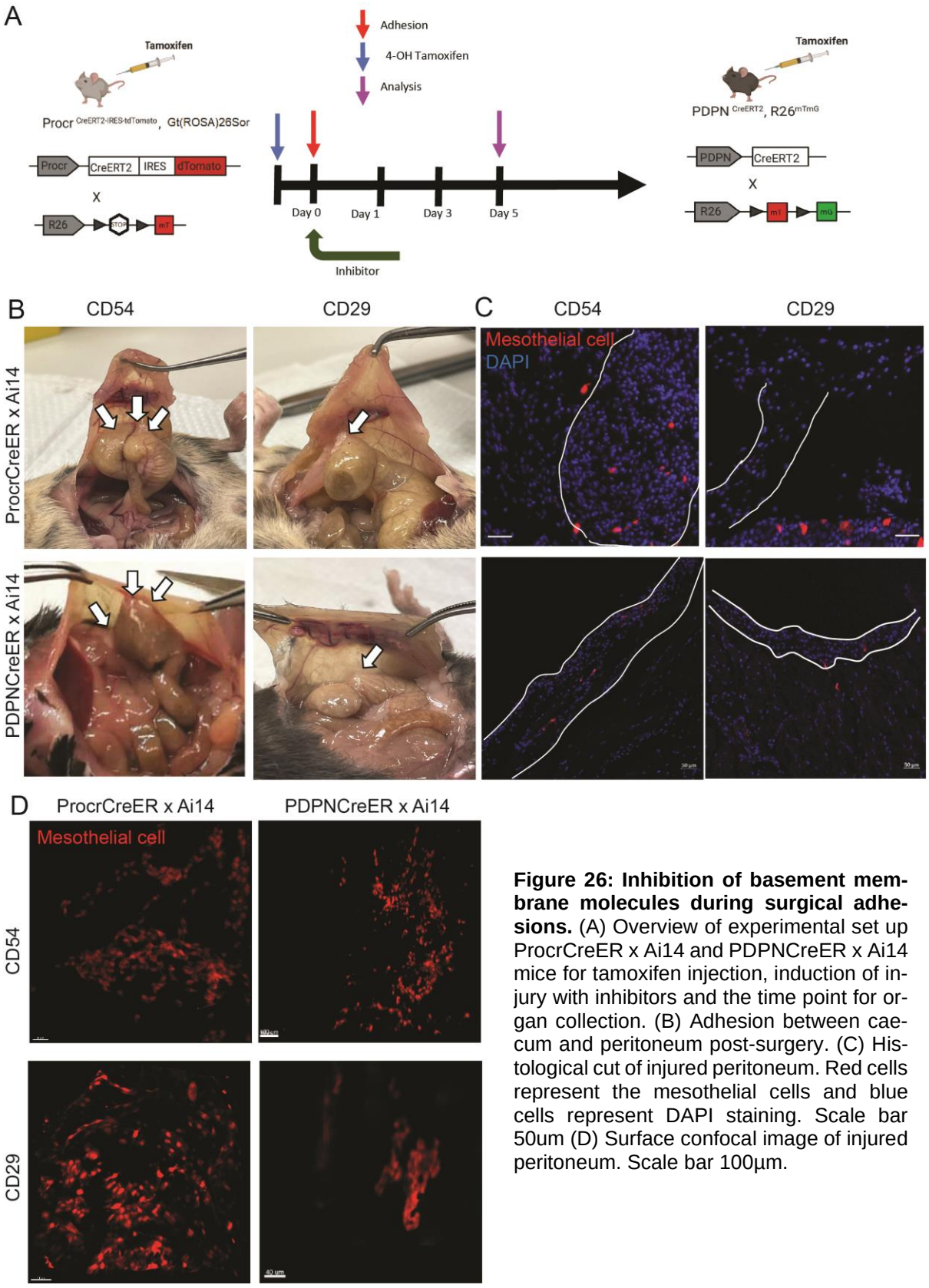

Figure 26: Inhibition of basement membrane molecules during surgical adhesions. (A) Overview of experimental set up ProcrCreER x Ai14 and PDPNCreER x Ai14 mice for tamoxifen injection, induction of injury with inhibitors and the time point for organ collection. (B) Adhesion between caecum and peritoneum post-surgery. (C) Histological cut of injured peritoneum. Red cells represent the mesothelial cells and blue cells represent DAPI staining. Scale bar 50um (D) Surface confocal image of injured peritoneum. Scale bar 100µm.

4. Discussion

Mesothelial cells surround all internal organs and play an essential role in tissue development, maintenance, and regeneration. Yet, the clonal capacity of this epithelium has not been addressed in detail. Here, we established two inducible transgenic mice models, PDPNCreER and ProcrCreER to study the cell clonality of mesothelial cells at two different scenarios: from post-natal development to aging, and from healthy to injury states. I investigated mesothelial cell clonality of 5 different organ systems such as the pleural and peritoneal cavity, the lung, the heart, the abdominal cavity, the liver, and the caecum. Initially, I investigated all the internal organs, and after complete analysis, I was able to capture the most significant data on mesothelial cell clones in the above-mentioned organs under the influence of 4-OH tamoxifen inducible mouse lines.

Under healthy conditions, I did not observe any changes in cell clonality, and low proliferation rate in mesothelial cells traced up to 1 year. Furthermore, cell division symmetry assessment showed that adult mesothelial cells undergo symmetric division. During post-natal developmental stages in neonates, I observed an increase in cell clonality, proliferation of mesothelial cells and determined that cells undergo symmetric and asymmetric cell division. Post injury, I observed an increase in cell clonality and proliferation of mesothelial cells.

4.1 Clonality change during aging

Single mesothelial cells were labelled on the organ surfaces and traced for up to 1 year. Then, I compared clones containing more than 5 cells for the collected organs at all the timepoints but did not observe abundant clones that are bigger than 5 cells and observed low proliferation rate in both Procr and PDPN positive mesothelial cells. These observation have been supported by an *in vitro* study where mesothelial cells were analyzed during homeostatic conditions and showed low proliferation rates (Steven E. Mutsaers, 2002). Furthermore, the clone sizes in both PDPN and Procr also remained similar and unchanged. Since mesothelial cells were already under the homeostatic condition, I did not observe change in the clonality up to 1 year of tracing. Interestingly, I observed an in-

crease in single cell numbers in some organs after 1 year. One possible explanation could be due to dissociation of clones into single cells which might have led to an increase in single cell number. This can be addressed by using the reporter line which has 4 colors (rainbow mouse) under the same promoters instead of using single color reporter mouse.

It has been suggested that mesothelial cells have the feature of mesenchymal stem cells (Lansley et al., 2011). Thus, my aim was to observe if mesothelial cells have differences in their cell division symmetry since, it is well known that stem cells undergo 2 different types of cell division; symmetric cell division to produce identical stem cells or 2 differentiated daughters, and asymmetric cell division to produce 1 differentiated daughter with identical stem cell properties (Morrison, Sean J & Kimble, 2006). Therefore, the percentages of clones containing even numbers of cells to clones which contain odd numbers of cells were compared and these were termed as cpDS as complete cell division symmetry (clones with even number of cells), unDS as incomplete cell division symmetry (clones with odd numbers of cells) and scDS as single cells. As an overview the percentages of cpDS-cpDS in all organs were more than cpDS-unDS. Thus, I concluded that adult mesothelial cells are mainly undergoing symmetric cell division like mesenchymal stem cells.

However, in the organ surfaces these their identical daughters in one clone were observed which led to my assumption that mesothelial cells are not undergoing EMT under homeostatic conditions. To further investigate their differentiation capacity over 1 year, these organs have been sectioned where 4-OH tamoxifen was injected 3 times in order to trace as many mesothelial cells as possible. Nevertheless, mesothelial cells were not observed inside organs and EMT was not addressed under homeostatic condition during adult stages. This led us to conclude that the adult mesothelium is not subjected to proliferation and differentiation. Moreover, the adult mesothelium post 1 year tracing did not migrate as described above.

4.2 Clonality during post-natal development

Following the adult stage, I investigated the clonality of mesothelium during post-natal development. To the best of my knowledge, mesothelial cells plays a crucial role in development and differentiation into different cell types (Koopmans & Rinkevich, 2018). My hypothesize was that clonality during post-natal development would be higher than adult stages since organs continue to develop and grow after birth. In order to address the above, pups were injected onset at post birth (P0) with low amount of 4-OH tamoxifen while, in P2 clones appeared bigger than 5 cells. Clonality of 2 days in post-natal development looked similar to 1 year in adult life. When I compared 3 time points (2-, 7- and 30- days), in 30 days the clone sizes increased up to 60 cells in the heart, 50 cells in the lung, 38 cells in the peritoneum and 26 cells in the liver. Therefore, I concluded that clonality during post-natal development and organ growth gradually increased and mesothelial cells might have role in organ growth and development. I decided to check if the clonal expansion was random around the organ surface, or the clonal expansion was in the direction of organ growth (data not shown). Our preliminary data showed that in the heart that the expansion of the clones have the similar directionality with the direction of the organ growth. To address this question, I decided to continue our analysis with all other organs. But our first findings were promising to say that clonal expansion did not take place randomly, but rather occurred in the direction of the organ growth. Like adult stages, Procr and PDPN positive cells did not show any differences in morphological change and in the expansion of clone sizes.

Like adult stage I wanted to check the cell division symmetry for the neonatal time point too. Number of cpDS-unDS percentage in Procr expressed peritoneum, liver and pdpn expressed peritoneum were more than cpDS-cpDS. cpDS-cpDS percentage in the rest of the organs were more than cpDS-unDS. Therefore, I concluded that adult mesothelial cells undergo asymmetric and symmetric cell division like pluripotent stem cells. This result enlightens that the neonatal mesothelial cells have stem cell like property during growth. During cell division, one cell proliferates to daughter cell and the other into differentiated cell. To address this part, I planned to do another set of experiments to check inside the organs and investigate their differentiation capacity to organ specific cell types. Another

approach would be to isolate the mesothelial cells from different organs at P0 and perform differentiation assays and staining such as alizarin red staining for osteogenic differentiation, alcian blue for chondrogenic differentiation, oil red for adipogenic differentiation. With this, I would be able to determine their differentiation capacity and pluripotency capacity during development and help us understand their role in development.

4.3 Clonality during injured conditions

After aging and development, the behavior of mesothelial cells upon injury was very important for us to investigate. Our hypothesis was that mesothelial cells upon injury will undergo activation and eventually will increase the cell clonality, since mesothelium has protective role upon injury. It is already known that mesothelial cells undergo activation upon inflammation and fibrosis and induce repair mechanism (Steven E. Mutsaers et al., 2015).

First, I investigated the mesothelial cell behavior in abdominal injury upon fibrosis (adhesions). I induced abdominal fibrosis via post-surgical adhesions established in our lab (Fischer et al., 2020). I observed that the formation of adhesion completes after 5 days post-surgery. As for proof of the adhesion formation, I determined the tissue cuts and observed thickening on the peritoneal mesothelial surfaces in both mouse lines. Therefore, I collected the samples after 5 days post-surgery from both the mouse lines and checked the adhesion surfaces and the surfaces near adhesion. I determined the parts far away from adhesion area and observed that the size of clones was low up to the single cell. I observed that the clonal expansion was drastically increased compared to the organs under homeostasis. With these findings, I prove that mesothelial cells migrate to the injury site and induce repair mechanism. Importance of mesothelial cells in the formation of adhesion have been mentioned above however, clinical studies on the role of mesothelium in adhesion are poorly studied. Following up, targeting mesothelial cells to prevent adhesion formation should be taken in consideration. There are some public single cell data on adhesion are available to investigate mesothelium specific genes during adhesion formation. List of these target genes can be used in *in vivo* studies to investigate the effect on adhesion formation. These findings mentioned above might help to establish targeted gene therapy

or medicines to use during abdominal surgeries to prevent post-surgical adhesions.

Next, I wanted to investigate the mesothelial cell behavior in pleural cavity upon fibrosis. I induced pleural injury via bleomycin installation into lungs. As a proof of our fibrosis model, I performed trichrome staining for collagen deposition. Bleomycin *in vivo* model is established to study IPF (Moeller et al., 2008). It has been established that pleural mesothelial cells differentiates into myofibroblast *in vitro* (Nasreen et al., 2009) and *in vivo* studies showed pleural mesothelial cells contributes to IPF (Liu et al., 2020). I hypothesized that the mesothelial clonality will increase upon bleomycin installation. Samples were collected at the end of the inflammation phase (day 10), at the peak of the fibrosis (day 14) and at the end of fibrosis (day 28). Clonality of mesothelial cells drastically increased at 28, at day 10 I saw the increase on the clonality but there were not such larger clones (bigger than 5 cells), I started observing larger clones at day 14 and at day 28 clones get larger. I concluded that the mesothelial cell clonality forms bigger clones after the peak of fibrosis and even continued to form bigger clones till the end of fibrosis. These findings above have been proven that mesothelial cell under stress condition in lungs become activated and were highly proliferative. Importance of mesothelium effect on IPF is poorly studied. With the findings mentioned above, the importance of mesothelium repair mechanism was shown. IPF is one of the major chronic lung diseases with the median survival rate up to 5 years after first diagnosis. Furthermore, there are limited IPF treatment options such as pirfenidone and nintedanib which slows the IPF progression but does not completely stop the fibrosis formation (Sauleda et al., 2018). Therefore, as a novel approach, the mesothelium can be targeted as a drug target for IPF treatment options.

Lastly, I check the mesothelial cell behavior upon abdominal inflammation. Non-infectious LPS model in rat has already been established and the mesothelial cell repair has been observed (Ito et al., 2017). Upon LPS treatment, I observed an expansion in cell clonality in peritoneum, liver and caecum compared to healthy control. LPS is one of the major microbial inducers for sepsis found in hospitals and the mortality rate associated is about 40% (Deng et al., 2013; Gabarin et al., 2021). Here, I showed that mesothelial cells are affected upon LPS induction and

undergo repair response by cell proliferation *in vivo*. Therefore, taken these findings into account, the mesothelial cells could be explored as a defense mechanism against LPS infection.

4.4 Role of basement membrane on clonality

Mesothelial cells attached to the basement membrane where they maintain their single layer arrangement and cover the organs. When there is a stimulation upon injury, the arrangement is disturbed and mesothelial cells are activated (Steven E. Mutsaers et al., 2015). I analyzed mesothelial single cell data upon injuries and observed the changes in basement membrane molecules Icam1 (CD54) and Itgb1 (CD29). Icam1 is a cell-cell attachment ligand, and itgb1 is a cell-matrix attachment ligand. I hypothesized that the loss of connection between mesothelial cell and basement membrane would induce mesothelial cell mobility. Study of basement membrane ligand loss gave us some insight of mesothelial cell clonal mechanism. Our approach was to check the importance of basement membrane during development and injury conditions. Therefore, I inhibited CD29 during development and did not observe any cell clones on the organ surfaces. Either there were patches of cell loss or single cells. Besides, when I inhibited CD54, during development clonality increased drastically and the cell number in clones increased up to 68 cells at P7 and the distribution of the clones were distributed randomly without any directionality. I concluded that the cell-matrix connection is important between mesothelial cell and basement membrane to maintain organ growth and proliferation, and cell-cell adhesion is important between mesothelial cells to maintain organization of organ growth and induce random proliferation of mesothelial cells. Thereafter, I inhibited these two molecules upon abdominal adhesion. Likely, development under CD54 inhibition, the cell clonality increased compared to control, and severity remained relatively same or even decreased compared to control. I also observed the differences in the peritoneum thickening on the mesothelial surfaces. CD54 inhibition increased the thickening as well the connection of other organs to the adhesion site increased. CD29 inhibition decreased the thickening as well as at the adhesion and there was no attachment between peritoneum and caecum. At this point, I came to conclusion that the cell-

cell connection is important between mesothelial cells to decrease the severity of injury and the cell-matrix connection is important for tissue repair.

In this thesis, I showed the mesothelium clonal change during different conditions, healthy, growth and injury. Lineage tracing of peritoneal mesothelium showed in postnatal and adult Wt1-Cre, Rosa26$^{LacZ/LacZ}$ mouse model, and they investigated the Wt1 expressing mesothelium contributes vascular smooth muscle during development in the intestine and mesentery only and the depletion of Wt1 expressing mesothelium is not required for maintaining the serosa (Wilm et al., 2021). Despite this thesis showed the importance of mesothelium to maintain homeostasis upon different injuries, not only peritoneal injury as well as pleural injury. Similar to previous work that mentioned above, postnatal mesothelium showed high clonality, but not only at intestines as well as at the other organs and the studies about directionality of mesothelial cells during growth showed their importance in organ growth. Besides, the two tamoxifen inducible mouse lines used in this study effectively trace mesothelial cells, which has not been broadly addressed previously. However, the mouse lines used in this study were not mesothelium specific, for example, PDPN is expressed by alveolar type 1 cells and Procr is expressed by lymphatics which is one of the limitations. To overcome this limitation, we were working on the single cell data to figure it out for each organ mesothelial specific markers, then if the mouse line for this specific gene is not exist, new transgenic line should be established. Overall, the importance of mesothelium concluded by this thesis but the molecular mechanism of mesothelium under the same conditions are still missing. To approach this, comprehensive single cell data analysis needs to be performed to find ligands between mesothelial cell to mesothelial cell, mesothelial cells to other cell types, and gene profiling under different injury conditions. Following up, *in vivo* studies, like upregulating or downregulating important ligands and genes can be performed to find molecular pathways that mesothelium involves. As a conclusion, findings in this thesis showed the importance of mesothelium, however they were poorly studied and understood. After *in vivo* findings, clinical research on mesothelium should be followed to prove their importance in abdominal fibrosis and inflammation, and lung fibrosis as discussed in the section 4.3.

5. Conclusion

Overall, two new transgenic mouse models were established in order to study mesothelial cell clonality at single cell resolution, in development, healthy and injury conditions. I conclude that the mesothelium and mesothelial cells plays an important role in development, injury and maintaining homeostasis primarily through a symmetric cell division status. Furthermore, mesothelial cells also have a capacity to act as stem cells.

References

Arai, H; Endo, M; Sasai, Y. et al. (1975). Histochemical demonstration of hyaluronic acid in a case of pleural mesothelioma. *Am. Rev. Respir. Dis.*, *111*, 699–702.

Astarita, J. L., Acton, S. E., & Turley, S. J. (2012). Podoplanin: Emerging functions in development, the immune system, and cancer. *Frontiers in Immunology*, *3*(SEP), 1–11. https://doi.org/10.3389/fimmu.2012.00283

Badia, J., Whawell, S., Scott-Coombes, D., Abel, P., Williamson, R., & Thompson, J. (1996). Peritoneal and systemic cytokine response to laparotomy. *Br J Surg*, *83*(3), 347–348.

Braun, K. M., & Diamond, M. P. (2014). The biology of adhesion formation in the peritoneal cavity. *Seminars in Pediatric Surgery*, *23*(6), 336–343. https://doi.org/10.1053/j.sempedsurg.2014.06.004

Deng, M., Scott, M. J., Loughran, P., Gibson, G., Sodhi, C., Watkins, S., Hackam, D., & Billiar, T. R. (2013). Lipopolysaccharide Clearance, Bacterial Clearance, and Systemic Inflammatory Responses Are Regulated by Cell Type–Specific Functions of TLR4 during Sepsis. *The Journal of Immunology*, *190*(10), 5152–5160. https://doi.org/10.4049/jimmunol.1300496

Ertürk, A., Becker, K., Jährling, N., Mauch, C. P., Hojer, C. D., Egen, J. G., Hellal, F., Bradke, F., Sheng, M., & Dodt, H.-U. (2012). Three-dimensional imaging of solvent-cleared organs using 3DISCO. *Nature Protocols*, *7*(11), 1983–1995. https://doi.org/10.1038/nprot.2012.119

Ferrandez-lzquierdo, A M.D.; Navarro-Fos, S. M.D.; Gonzalez-Devesa, M. M.D.; Gil-Benso, R. Ph.D.; Llombart-Bosch, A. (1994). Immunocytochemical typification of mesothelial cells in effusions: In vivo and in vitro models. *Diagnostic Cytopathology*, *10*(3), 256–262. https://doi.org/10.1002/dc.2840100313

Fischer, A., Koopmans, T., Ramesh, P., Christ, S., Strunz, M., Wannemacher, J., Aichler, M., Feuchtinger, A., Walch, A., Ansari, M., Theis, F. J., Schorpp, K., Hadian, K., Neumann, P. A., Schiller, H. B., & Rinkevich, Y. (2020). Post-surgical adhesions are triggered by calcium-dependent membrane bridges between mesothelial surfaces. *Nature Communications*, *11*(1). https://doi.org/10.1038/s41467-020-16893-3

Gabarin, R. S., Li, M., Zimmel, P. A., Marshall, J. C., Li, Y., & Zhang, H. (2021). Intracellular and Extracellular Lipopolysaccharide Signaling in Sepsis: Avenues for Novel Therapeutic Strategies. *Journal of Innate Immunity*, *13*(6), 323–332. https://doi.org/10.1159/000515740

Gotloib, L; Shostack, A; Jaichenko, J. (1988). Ruthenium-red- stained anionic charges of rat and mice mesothelial cells and basal lamina: The peritoneum is a negatively charged dialyzing membrane. *Nephron*, *48*, 65– 70.

Habiel, David M; Hogaboam, C. M. (2017). Heterogeneity of Fibroblasts and Myofibroblasts in Pulmonary Fibrosis. *Current Pathobiology Reports Volume*, *5*, 101–110.

Herrick, S. E., & Mutsaers, S. E. (2004). Mesothelial progenitor cells and their potential in tissue engineering. *International Journal of Biochemistry and Cell Biology*, *36*(4), 621–642. https://doi.org/10.1016/j.biocel.2003.11.002

Herrick, S. E., & Wilm, B. (2021). Post-surgical peritoneal scarring and key molecular mechanisms. *Biomolecules*, *11*(5), 1–17. https://doi.org/10.3390/biom11050692

Hesseldah,l H; Larsen, J. (1969). Ultrastructure of human yolk sac: endoderm, mesenchyme, tubules and mesothelium. *Am J Anat.*, *126*(3), 315–335. https://doi.org/10.1002/aja.1001260306

Holmdahl, L. (1997). The role of fibrinolysis in adhesion formation. *Eur J Surg Suppl.*, *577*, 24–31.

Horejs, C.-M. (2016). Basement membrane fragments in the context of the epithelial-to-mesenchymal transition. *European Journal of Cell Biology*, *95*(11), 427–440.

Ishihara, Tokuhiro; Ferrnas, Victor J; Jones, Michael; Boyce, Steven; Kawanami, Oichi; Roberts, W. C. (1980). Histologic and ultrastructural features of normal human parietal pericardium. *The American Journal of Cardiology*, *46*(5), 744–753. https://doi.org/10.1016/0002-

9149(80)90424-5

Ito, Y., Kinashi, H., Katsuno, T., Suzuki, Y., & Mizuno, M. (2017). Peritonitis-induced peritoneal injury models for research in peritoneal dialysis review of infectious and non-infectious models. *Renal Replacement Therapy*, *3*(1), 16. https://doi.org/10.1186/s41100-017-0100-4

Jantz, M. A., & Antony, V. B. (2008). Pathophysiology of the pleura. *Respiration*, *75*(2), 121–133. https://doi.org/10.1159/000113629

Jones, L., Gardner, M., Catterall, J., & Turner, G. (1995). Hyaluronic acid secreted by mesothelial cells: A natural barrier to ovarian cancer cell adhesion. *Clin. Exp. Metastasis*, *13*, 373–380.

Kalluri, R., & Neilson, E. G. (2003). Epithelial-mesenchymal transition and its implications for fibrosis. *Journal of Clinical Investigation*, *112*(12), 1776–1784. https://doi.org/10.1172/JCI200320530

Kalluri, R., & Weinberg, R. a. (2009). Review series The basics of epithelial-mesenchymal transition. *Journal of Clinical Investigation*, *119*(6), 1420–1428. https://doi.org/10.1172/JCI39104.1420

Kaminski, N., Belperio, J. A., Bitterman, P. B., Chen, L., Chensue, S. W., Choi, A. M. K., Dacic, S., Dauber, J. H., Bois, R. M., Enghild, J. J., Fattman, C. L., Grutters, J. C., Haegens, A., Hanford, L. E., Heintz, N., Henson, P. M., Hogaboam, C., Kagan, V. E., Keane, M. P., … Noble, P. W. (2003). *Idiopathic Pulmonary Fibrosis*. *29*. https://doi.org/10.1165/rcmb.2003-0159SU

Koopmans, T., & Rinkevich, Y. (2018). Mesothelial to mesenchyme transition as a major developmental and pathological player in trunk organs and their cavities. *Communications Biology*, *1*(1), 170. https://doi.org/10.1038/s42003-018-0180-x

Lachaud, C. C., Pezzolla, D., Domínguez-Rodríguez, A., Smani, T., Soria, B., & Hmadcha, A. (2013). Functional Vascular Smooth Muscle-like Cells Derived from Adult Mouse Uterine Mesothelial Cells. *PLoS ONE*, *8*(2), 1–17. https://doi.org/10.1371/journal.pone.0055181

Lachaud, C. C., Rodriguez-Campins, B., Hmadcha, A., & Soria, B. (2015). Use of mesothelial cells and biological matrices for tissue engineering of simple epithelium surrogates. *Frontiers in Bioengineering and Biotechnology*, *3*(AUG). https://doi.org/10.3389/fbioe.2015.00117

Lansley, S. M., Searles, R. G., Hoi, A., Thomas, C., Moneta, H., Herrick, S. E., Thompson, P. J., Mark, N., Sterrett, G. F., Prêle, C. M., & Mutsaers, S. E. (2011). Mesothelial cell differentiation into osteoblast- and adipocyte-like cells. *Journal of Cellular and Molecular Medicine*, *15*(10), 2095–2105. https://doi.org/10.1111/j.1582-4934.2010.01212.x

LeBleu, V. S., MacDonald, B., & Kalluri, R. (2007). Structure and function of basement membranes. *Experimental Biology and Medicine*, *232*(9), 1121–1129. https://doi.org/10.3181/0703-MR-72

Li, F., Davenport, A., & Robson, R. (1998). Leukocyte migration across human peritoneal mesothelial cells is dependent on directed chemokine secretion and ICAM-1 expression. *Kidney Int.*, *54*, 2170–2183.

Liu, F., Yu, F., Lu, Y. Z., Cheng, P. P., Liang, L. M., Wang, M., Chen, S. J., Huang, Y., Song, L. J., He, X. L., Xiong, L., Xin, J. B., Ma, W. L., & Ye, H. (2020). Crosstalk between pleural mesothelial cell and lung fibroblast contributes to pulmonary fibrosis. *Biochimica et Biophysica Acta - Molecular Cell Research*, *1867*(11), 118806. https://doi.org/10.1016/j.bbamcr.2020.118806

Menzies, D., & Ellis, H. (1990). Intestinal obstruction from adhesions--how big is the problem? *Annals of the Royal College of Surgeons of England*, *72*(1), 60–63. http://www.pubmedcentral.nih.gov/articlerender.fcgi?artid=2499092&tool=pmcentrez&rendertype=abstract

Mironov, V. A., Gusev, S. A., & Baradi, A. F. (1979). Mesothelial stomata overlying omental milky spots: Scanning electron microscopic study. *Cell and Tissue Research*, *201*(2), 327–330. https://doi.org/10.1007/BF00235068

Moeller, A., Ask, K., Warburton, D., Gauldie, J., & Kolb, M. (2008). The bleomycin animal model: A useful tool to investigate treatment options for idiopathic pulmonary fibrosis? *International Journal of Biochemistry and Cell Biology*, *40*(3), 362–382. https://doi.org/10.1016/j.biocel.2007.08.011

Moore, K., Persaud, T. & Torchia, M. B. (2019). *Before We Are Born. Essentials of Embryology and Birth Defects* (10th ed.). Elsevier.

Morrison, Sean J & Kimble, J. (2006). Asymmetric and symmetric stem-cell divisions in development and cancer. *Nature*, *441*, 1068–1074.

Mubarak, K. K., Montes-Worboys, A., Regev, D., Nasreen, N., Mohammed, K. A., Faruqi, I., Hensel, E., Baz, M. A., Akindipe, O. A., Fernandez-Bussy, S., Nathan, S. D., & Antony, V. B. (2012). Parenchymal trafficking of pleural mesothelial cells in idiopathic pulmonary fibrosis. *European Respiratory Journal*, *39*(1), 133–140. https://doi.org/10.1183/09031936.00141010

Munoz-Chapuli, R; Perez-Pomares, JM; Macias, D. et al. (1999). Differentiation of hemangioblasts from embryonic mesothelial cells? A model on the origin of the vertebrate cardiovascular system. *Differentiation*, *64*, 133–41.

Mutsaers, E. E., Whitaker, D., & Papadimitriou, J. M. (1996). Changes in the concentration of microvilli on the free surface of healing mesothelium are associated with alterations in surface membrane charge. *Journal of Pathology*, *180*(3), 333–339. https://doi.org/10.1002/(SICI)1096-9896(199611)180:3<333::AID-PATH659>3.0.CO;2-Y

Mutsaers, S. E., Bishop, J. E., McGrouther, G., & Laurent, G. (1997). Mechanisms of tissue repair: From wound healing to fibrosis. *The International Journal of Biochemistry & Cell Biology, 29*(1), 5–17.

Mutsaers, Steven E. (2002). Mesothelial cells: Their structure, function and role in serosal repair. *Respirology*, *7*(3), 171–191. https://doi.org/10.1046/j.1440-1843.2002.00404.x

Mutsaers, Steven E. (2004). The mesothelial cell. *International Journal of Biochemistry and Cell Biology*, *36*(1), 9–16. https://doi.org/10.1016/S1357-2725(03)00242-5

Mutsaers, Steven E., Birnie, K., Lansley, S., Herrick, S. E., Lim, C. B., & Prêle, C. M. (2015). Mesothelial cells in tissue repair and fibrosis. *Frontiers in Pharmacology*, *6*(MAY), 1–12. https://doi.org/10.3389/fphar.2015.00113

Mutsaers, Steven E., Whitaker, D., & Papadimitriou, J. M. (2002). Stimulation of mesothelial cell proliferation by exudate macrophages enhances serosal wound healing in a murine model. *American Journal of Pathology*, *160*(2), 681–692. https://doi.org/10.1016/S0002-9440(10)64888-2

Mutsaers, Steven Eugene, Prêle, C. M. A., Pengelly, S., & Herrick, S. E. (2016). Mesothelial cells and peritoneal homeostasis. *Fertility and Sterility*, *106*(5), 1018–1024. https://doi.org/10.1016/j.fertnstert.2016.09.005

Nasreen, N., Mohammed, K. A., Mubarak, K. K., Baz, M. A., Akindipe, O. A., Fernandez-Bussy, S., & Antony, V. B. (2009). Pleural mesothelial cell transformation into myofibroblasts and haptotactic migration in response to TGF-β1 in vitro. *American Journal of Physiology - Lung Cellular and Molecular Physiology*, *297*(1), 115–124. https://doi.org/10.1152/ajplung.90587.2008

Odor, D. L. (1954). Observations of the rat mesothelium with the electron and phase microscopes. *American Journal of Anatomy*, *95*(3), 433–465. https://doi.org/10.1002/aja.1000950304

Perez-Pomares, J. M., Carmona, R., González-Iriarte, M., Atencia, G., Wessels, A., & Muñoz-Chapuli, R. (2002). Origin of coronary endothelial cells from epicardial mesothelium in avian embryos. *International Journal of Developmental Biology*, *46*(8), 1005–1013. https://doi.org/035083

Pérez-Pomares, J. M., Carmona, R., González-Iriarte, M., Macías, D., Guadix, J. A., & Muñoz-Chápuli, R. (2004). Contribution of Mesothelium-Derived Cells to Liver Sinusoids in Avian Embryos. *Developmental Dynamics*, *229*(3), 465–474. https://doi.org/10.1002/dvdy.10455

Pozzi, A., Yurchenco, P. D., & Iozzo, R. V. (2017). The nature and biology of basement membranes. *Matrix Biology*, *57–58*, 1–11. https://doi.org/10.1016/j.matbio.2016.12.009

Raftery, A. T. (1973). Regeneration of parietal and visceral peritoneum in the immature animal: A light and electron microscopical study. *British Journal of Surgery*, *60*(12), 969–975.

Rao, L. Vijaya Mohan; Esmon, Charles T.; Pendurthi, U. R. (2014). Endothelial cell protein C receptor: a multiliganded and multifunctional receptor. *Blood*, *124*(10), 153–1562.

Rennard, S., Jaurand, M., Bignon, J., Kawanami, O., Ferrans, V., Davidson, J., & Crystal, R. (1984). Role of pleural mesothelial cells in the production of the submesothelial connective tissue matrix of lung. *Am Rev Respir Dis.*, *130*(2), 267–274. https://doi.org/10.1164/arrd.1984.130.2.267

Rinkevich, Y., Montoro, D. T., Contreras-Trujillo, H., Harari-Steinberg, O., Newman, A. M., Tsai, J. M., Lim, X., Van-Amerongen, R., Bowman, A., Januszyk, M., Pleniceanu, O., Nusse, R., Longaker, M. T., Weissman, I. L., & Dekel, B. (2014). In vivo clonal analysis reveals lineage-restricted progenitor characteristics in mammalian kidney development, maintenance, and regeneration. *Cell Reports*, *7*(4), 1270–1283. https://doi.org/10.1016/j.celrep.2014.04.018

Rinkevich, Y., Mori, T., Sahoo, D., Xu, P. X., Bermingham, J. R., & Weissman, I. L. (2012). Identification and prospective isolation of a mesothelial precursor lineage giving rise to smooth muscle cells and fibroblasts for mammalian internal organs, and their vasculature. *Nature Cell Biology*, *14*(12), 1251–1260. https://doi.org/10.1038/ncb2610

Roth, J. A. (1973). Ultrahistochemical demonstration of saccha- ride components of complex carbohydrates at the alve- olar cell surface and at the mesothelial cell surface of the pleura visceralis of mice by means of concanavalin. *Exp. Pathol.*, *8*, 157–67.

Sauleda, J., Núñez, B., Sala, E., & Soriano, J. (2018). Idiopathic Pulmonary Fibrosis: Epidemiology, Natural History, Phenotypes. *Medical Sciences*, *6*(4), 110. https://doi.org/10.3390/medsci6040110

Tiedemann, K. (1976). On the yolk sac of the cat. Endoderm and mesothelium. *Cell Tissue Res.*, *173*(1), 109–127.

Tsai, J., Sinha, R., Seita, J., Fernhoff, N., Christ, S., Koopmans, T., Krampitz, G., McKenna, K., Xing, L., Shoham, M., McCracken, M., Joubert, L., Gordon, S., Poux, N., Wernig, G., Norton, J., Sandholzer, M., Sales, J., Weissman, I., & Rinkevich, Y. (2017). Adhesions are derived from hypoxia responsive MSLN+ mesothelial cells and are resolved via targeted therapies. *Science Translational Medicine*.

Von Recklinghausen, F. (1863). Zur fettresorption. *Arch. Pathol. Anat*, *24*, 172–208.

Wang, N. (1974). The regional difference of pleural mesothelial cells in rabbits. *Am. Rev. Respir. Dis*, *110*, 623– 633.

Wilm, T. P., Tanton, H., Mutter, F., Foisor, V., Middlehurst, B., Ward, K., Benameur, T., Hastie, N., & Wilm, B. (2021). Restricted differentiative capacity of Wt1-expressing peritoneal mesothelium in postnatal and adult mice. *Scientific Reports*, *11*(1), 1–15. https://doi.org/10.1038/s41598-021-95380-1

Zheng, M., & Yamada, K. M. (2019). *Using Sliding Focal Adhesions Driven By a Contractile Winch*. 1–42.

Zolak, J. S., Jagirdar, R., Surolia, R., Karki, S., Oliva, O., Hock, T., Guroji, P., Ding, Q., Liu, R. M., Bolisetty, S., Agarwal, A., Thannickal, V. J., & Antony, V. B. (2013). Pleural mesothelial cell differentiation and invasion in fibrogenic lung injury. *American Journal of Pathology*, *182*(4), 1239–1247. https://doi.org/10.1016/j.ajpath.2012.12.030

Acknowledgements

On the way of my scientific career there were lot of ups and downs, disappointments, and sadness but there were many people and occasions to make me stand up again and continue my journey. Now we have come to the end of this journey, and I am so proud of myself.

I was born in Istanbul and had an awesome childhood. I am always so grateful that I had one of the best educations thought my life. As a family we had struggles, ups and downs, but we never gave up, they never let me give up. During science high school I never thought I would continue as biologist to be honest I had always the worse grades in Biology 😊, but I became one. I am happy to choose this area, people I met on the way. When I look back, I have no regrets but gratefulness.

First, I would like to thank my supervisor Dr. Yuval Rinkevich for giving me an opportunity to do my PhD Thesis in his lab. I would also like to thank him for his guidance and constant support during my PhD work. I have learned a lot from him, and I became an independent scientist. I will carry all the knowledge and experiences I gained during these 4 years with me. I am so grateful that my way crossed with Yuval, and I had an opportunity to work with him. Thank you for the inspiration and motivation to pursue my PhD. Thank you very much Yuval 😊

I would also like to thank my Thesis Advisory Committee members Prof. Dr. med Jürgen Behr and PD Dr. Claudia Staab-Weijnitz for their support and advice throughout my PhD journey. I always took their advice into account and improved myself and my project to the next step. I would like to thank PD Dr. Claudia Staab-Weijnitz for CPC Research School training and activities during these 4 years. They were always fun to attend and a lot of knowledge to take with me.

I would also like to thank our collaboration partner Dr. Carsten Marr. Thank you for your input with the computational analysis and statistical analysis. It was always nice to have meetings together, I learned a lot from you, and I will carry all the knowledge whole my career.

Thanks to Tim Koopmans, for his support since my master's degree and throughout my PhD. Thank you for always being available whenever I had questions and thank you for answering everything with patience. Thank you for being a great colleague and friend. Thanks to Adrian Fischer, for his great supervision during my master thesis and always being there to talk and discuss during my PhD. Thank you for being a great colleague. Thanks to Tankut Gökhan Güney, for his great support during the time we shared together in the same group. It was so nice to have a colleague to speak in Turkish around (sometimes me to express my feeling much easier in my mother tongue, you know 😊). It was always nice spend time with while drinking Turkish coffee and talk about your little daughter

Ayla. You are a great colleague; it was always nice to work with you and do experiments together. I gained a great friend.

Thanks to Andy Qarri, for being a great friend. It was so nice to share the office space together even though we used to fight a lot in the beginning 😉 I always appreciated your advice about science as well as about life. I am glad to earn a trustworthy friend. I will never forget the fun we also had outside the lab. Thank you for being there whenever I need to talk and thank you for listening to me with patience. Thanks to Haifeng Ye, for being a great lab partner and friend. We always struggled with similar things through the PhD journey, but we had always supported each other by heart. It was memorable to go conference in Lyon, France together. I am happy to earn friend like you and I hope we will be in touch even we will be in different countries 😉 Thanks to Vijayanand Rajendaren, for being a great friend. I will never forget the time we spent in the lab working until late times and talking about life. It was great to have you beside me since my master's project. Thanks for being there for me and the times we spent together. Thanks to Bikram Dasgupta for being a nice friend and colleague, our friendship started late but it evolved eventually. It was fun to work together and do experiments as well as the times we spent outside lab. Thanks to Donovan Correa-Gallagos for his patience whenever I ask questions, your scientific input always helped me, and I will carry all the scientific that I learned from you with me. It was also honor for me to work with you in the same project. Thanks to Martin Mück-Häusl for his scientific input and his support on my project. Thanks to Juliane Wannemacher for helping me to learn *in vivo* works, TVA writing and all the training. Thanks to Yiqun Su for being a great project partner and office partner. I was always happy to share same place with you, even though you were always using my PC when I was not around😉 Thanks to Dongsheng Jiang for helping me with the issues of animal experiments. Your suggestions were always very helpful. Thanks to Natalja Ring for bringing cake and chocolates to cheer us up 😊 Thanks to Ruoxuan Dai and Yue Lin for being nice friends and smiling all the time 😊 Thanks to Christoph Deisenhofer for helping me with genotyping duty 😉

I would like to thank all my former and rest of the current lab members, Subhasree Dutta, Disha Shenai, Fanzhu Zeng, George Vogelaar, Jiakuan Zhao, Jiazheng Lai, Li Wan, Mahesh Gouda, Maria Chiara Bosello, Meng Liu, Pushkar Ramesh, Qing Yu, Ravinder Kandi, Robert Koplin, Ruiji Guo, Ryo Ichijo, Safoune Kadri, Sandra Schiener, Shaohua Zhu, Shaoping Hu, Shruthi Kalgudde Gopal, Simon Christ, Wei Han, Xiangyu Zhang, Young Hwa. I had a great time with all of you, thanks for making PhD time fun for me.

I would like to thank all my friends who supported me during my hard times and were happy with me during my happy times. Thanks to Mert Akgündüz for being such a great person and friend. Our journey together from Istanbul to Oxford to Munich was always fun. I am so lucky to have you in my life, thanks for your

support and never letting me down during my sad times. Our memorable times will never get old, and we will make more memories together. Thanks to Ceylan Onursal, for being a great friend. Your support with life was valuable, and the time we spent together will never be forgotten. We will continue travelling and make new funny memories. Thanks for always being beside me.

Now I would like to take a moment and thank my boyfriend Ashesh Chakraborty. Thank you for being such a great person, I love you and I will always love you. We met during our PhD, and we came over with the struggles together. We always supported each other, and we always learned from each other. This PhD journey finished here and now we will continue with the new ones.

Last but not least, I would like to thank my family. My mother, father, brother, sister-in-law and our little new member my niece. You always supported me whole my career, never let me feel down and never let me give up. Without you and your support I would never achieve success. Thank you for always being there for me and not letting me feel alone. I am so happy and glad to have a family such you. I always feel lucky to have a family like you. Sizi çok seviyorum iyi ki varsınız!